Defence Research and Development Canada
Recherche et développement pour la défense Canada

DEFENCE R&D DÉFENSE

Detection of Frequency Hopping Signals in Digital Wideband Data

William J.L. Read

Defence R&D Canada - Ottawa
TECHNICAL REPORT
DRDC Ottawa TR 2002-162
December 2002

Canada

Detection of frequency hopping signals in digital wideband data

William J.L. Read

Defence R&D Canada – Ottawa

Technical Report

DRDC Ottawa TR 2002-162

December 2002

Abstract

In this report, a number of approaches to detect a frequency hopped signal in digital wideband data were investigated, both theoretically and through computer simulations. These approaches included the FFT, the polyphase filter, and the periodogram, plus variants of the these approaches using windowing functions and frequency smoothing. Additionally, the maximum likelihood approach was included as a benchmark for detection performance. The main purpose of the investigation was to determine the best approach for detecting a frequency hopped signal in wideband data in the presence of noise. The effect of interference from other inband signals was considered, and an assessment of the number of computations required for each approach was also carried out.

Résumé

Dans ce rapport plusieurs approches, pouvant être utilisées pour la résolution du problème de détection des signaux à sauts de fréquence dans le cas de données numériques à bande large, furent examinées en détail, à la fois théoriquement et au moyen de simulations par ordinateur. Ces approches emploient la transformée de Fourier rapide, le filtre polyphase et le périodogramme, ainsi que des variations de ces méthodes utilisant des fonctions fenêtres et de lissage de fréquence. En plus, la méthode de maximum de vraisemblance est incluse dans ce rapport, en temps que point de réference pour la performance de détection. Le but premier de cette recherche a été de déterminer la meilleure approche pour détecter un signal à sauts de fréquence, dans le cas de données à bande large, en présence de bruit de fond. Les effets dus aux interférences, générées par d'autre signaux existant à l'intérieur de la bande passante, furent considérés. Une évaluation du nombre de calculs requis pour chacune des différentes approches fut aussi menée à bonne fin.

This page intentionally left blank.

Executive summary

The introduction of wideband receivers to modern Communications Electronics Support Measures systems, as well as the ongoing technological advances in computer systems, has made it possible to apply better and better approaches to the problem of signal detection and estimation. Of particular interest is the detection and estimation of the short duration signals (hops) generated by frequency hopping radios, which have begun to proliferate on the modern battlefield.

Using wideband receivers, the frequency band over which a frequency hopping radio is operating can be monitored and every hop recorded. Unfortunately, every other signal in this band, plus noise, will also be recorded, making it more difficult to find and track the targeted hopping signal, especially when these other signals are stronger.

To this end, a number of approaches that can detect a frequency hopped signal in digital wideband data were investigated, both theoretically and using computer simulations. These approaches included the FFT, the polyphase filter, and the periodogram, plus variants of the these approaches using windowing functions and frequency smoothing. Additionally, the maximum likelihood approach was included as a benchmark for detection performance. This approach, however, is not useful for practical applications, as it requires exact knowledge of the modulation envelope, which would not be available.

The main purpose of the investigation was to determine the best approach for detecting a frequency hopped signal in wideband data in the presence of noise. Generally, detection performance is related to the size of the observation window (the number of input samples used to make the detection assessment for a given time instance), where longer is better. The best performance is achieved when the observation window matches the hop duration, such as for the periodogram, or when the data containing the entire hop is used to generate a single FFT result, which is then smoothed in frequency (called the match frequency smoothed FFT or MFS-FFT approach here).

The investigation also highlighted other issues which have important practical implications. The first issue is sidelobe suppression. Sidelobes give rise to measurable signal power at frequencies outside the expected range of the signal. This unwanted signal power can mask weaker signals, making them impossible to detect. There are three methods that can be used to suppress the sidelobes: increase the FFT size, use a windowing function, or go to a polyphase filter technique. Using a polyphase filter yields the greatest benefit, while increasing the FFT size can also be moderately effective. The use of windowing functions, unfortunately, leads to poorer detection performance.

The second issue is processing time. Processing time tends to be a function of the number of frequency channels used: the greater the number of channels, the longer the processing time. The result is that approaches employing frequency smoothing are slow, with the MFS-FFT approach being the slowest since it involves the calculation of

the largest number of frequency channels. The shortest processing time is required for the single channel FFT approach, followed closely by the periodogram approach, both of which also used the fewest number of frequency channels. Windowing functions for these two approaches lead to slightly longer processing times.

Generally, the selection of the best detection approach for a given application results in a trade-off between performance and processing time. In terms of processing time, the FFT single channel or periodogram approaches with or without windows are the fastest. For state-of-the-art wideband receiving systems and realtime processing requirements, they may, in fact, be the only choices. In terms of performance, the MFS-FFT approach is the best choice when both detection and sidelobe suppression are taken into account. It is possible to detect frequency hopped signals at far lower signal-to-noise ratios than any of the other approaches investigated except the periodogram. The periodogram approach has the same or slightly worse detection performance than the MFS-FFT approach, but poorer sidelobe performance.

Another consideration that may affect the choice of approach is integration with other applications. From the ESM perspective, detection of a hop signal is not usually sufficient information. Estimation of hop parameters such as the hop signal bandwidth, start time, duration, and bearing are also of interest, so that the signal can be tracked in frequency and time. Detection approaches that integrate well with these estimation requirements, without sacrificing too much processing speed or performance, will be more desirable.

Compared to the ultimate performance of the maximum likelihood apporach, the MFS-FFT and periodogram approaches still fall well short. It may also be possible to estimate the hop amplitude profile and the frequency profile from initial hop detections, and then incorporate this information into the detection process to improve performance. Alternatively, higher order statistical methods might also be incorporated to take advantage of the higher order statistical properties of man-made signals. In any case, more research needs to be done in this area to investigate and/or develop approaches which can provide improved frequency hop detection performance for practical applications.

Read, W.J.L. 2002. Detection of frequency hopping signals in digital wideband data. DRDC Ottawa TR 2002-162. Defence R&D Canada – Ottawa.

Sommaire

L'introduction de récepteurs à large bande, dans le domaine des systèmes de communication de mesures de soutien électronique, aussi bien que les progrès technologiques continuels dans le domaine des systèmes d'ordinateurs, a rendu possible l'emploi d'approches allant toujours en s'améliorant pour solutionner les problèmes de détection de signaux aussi bien que d'estimation. Un intérêt particulier est porté sur la détection et l'estimation des signaux de courte durée (bonds) générés par des radios à sauts de fréquence qui ont commencé à proliférer sur les chanps de bataille modernes.

L'utilisation de récepteurs à large bande permet de controler la bande de fréquence sur laquelle une radio à sauts de fréquence opère et aussi d'enregistrer tous les bonds émis. Malheureusement, tout autre signal existant dans cette bande passante, ainsi que du bruit de fond, seront également enregistrés augmentant ainsi la difficulté de trouver et de poursuivre le signal cible, tout spécialement quand ces autres signaux sont forts.

Dans ce but plusieurs approches, pouvant être utilisées pour la résolution du problème de détection des signaux à sauts de fréquence dans le cas de données numériques à bande large, furent examinées en détail, à la fois théoriquement et au moyen de simulations par ordinateur. Ces approches emploient la transformée de Fourier rapide, le filtre polyphase et le périodogramme, ainsi que des variations de ces méthodes utilisant des fonctions fenêtres et de lissage de fréquence. En plus, la méthode de maximum de vraisemblance est incluse dans ce rapport, en temps que point de référence pour la performance de détection. Toutefois, cette derniere approche n'a aucune utilisation pratique car la connaissance exacte de l'enveloppe de la modulation est requise, cette dernière information n'étant pas disponible.

Le but premier de cette recherche a été de déterminer la meilleure approche pour détecter un signal à sauts de fréquence, dans le cas de données à bande large, en présence de bruit de fond. Généralement, la performance de détection est reliée à la grandeur de la fenêtre d'observation (le nombre d'échantillons d'entrée utilisés pour évaluer la performance de détection à un instant donné). Plus grande est la fenêtre d'observation, meilleure sera la performance de détection. La meilleure performance est obtenue quand la longueur de la fenêtre d'observation concorde avec la durée du bond, comme dans le cas du périodogramme, ou quand toutes les données contenues dans le bond sont utilisées pour générer un résultat de transformée de Fourier rapide unique. Le spectre de fréquence ainsi obtenu est ensuite lissé (cette approche est appellée transformée de Fourier rapide à fréquence adaptée et lissée).

Cette recherche mit aussi en évidence d'autres problèmes qui ont des implications pratiques non négligables. Un de ces problèmes est l'élimination des lobes secondaires. Les lobes secondaires produisent une puissance mesurable à des fréquences situées à l'extérieur de l'intervalle prévu pour ce signal. Cette puissance parasite peut masquer des signaux plus faibles les rendant ainsi impossibles à détecter. Il existe trois méthodes pour éliminer les lobes secondaires: accroitre la taille de la transformée de Fourier rapide, utiliser une fonction fenêtre, ou se servir d'une technique de filtrage polyphase.

Les meilleurs résultats sont obtenus en utilisant un filtre polyphase, quoique l'augmentation de la taille de la transformée de Fourier rapide peut aussi s'avérer modérément efficace. Malheureusement l'utilisation de fonctions fenêtres produit une performance de détection plus faible.

Le second problème est relié au temps de traitement. Le temps de traitement tend a être fonction du nombre de voies de fréquence utilisées. Plus grand est ce nombre de voies de fréquence plus long sera le temps de traitement. Le résultat de tout ceci est que les approches utilisant le lissage de fréquence sont lentes, la transformée de Fourier rapide à fréquence adaptée et lissée étant la pire a cause du plus grand nombre de voies de fr'equence utilsées pour le traitement. Le temps de traitement le plus court est requis par l'approche utilisant la transformee de Fourier rapide sur une voie de fréquence unique. Dans cet ordre d'idées l'approche utilisant le périodogramme suit de près, ces deux approches utilisant le plus petit nombre de voies de fréquence. L'utilisation de fonctions fenêtres pour ces deux approches augmente légèrement le temps de traitement.

D'une façon générale sélectionner la meilleure approche de détection pour une utilisation donnée revient à choisir entre performance et temps de traitement. En terme de temps de traitement, les approches utilisant soit la transformée de Fourier rapide sur une voie de fréquence unique, soit le périodogramme, avec ou sans fonction fenêtre, sont sans contredit les plus rapides. Pour des systèmes de réception à large bande à la fine pointe de la technologie et aussi pour les exigeances du traitement en temps réel, elle constitue en fait le seule option possible. Si l'accent est mis sur la performance, la transformée de Fourier rapide à fréquence adaptée et lissée constitue le meilleur choix, quand à la fois détection et élimination des lobes secondaires doivent être pris en considération. En terme de détection , il est possible de déceler des signaux à sauts de fréquence pour des rapports signal sur bruit bien plus bas que pour n'importe quelle autre approche étudiée, à l'exception toutefois du périodogramme. L'approche utilisant le périodogramme présente une performance équivalente ou légèrement inférieure à celle de la transformée de Fourier rapide à fréquence adaptée et lissée. En terme d'élimination des lobes secondaires sa performance est plus faible.

Une autre raison peut influencer le choix de l'approche, et c'est son intégration avec d'autres fonctionalités. Du point de vue des mesures de soutien électronique, déceler un signal à sauts de fréquence ne contitue pas en soi un résultat suffisant. L'évaluation de paramètres du bond tels la largeur de bande, le temps de commencement, la durée, et l'azimuth est aussi importante, de telle sorte que le signal peut être à la fois suivi en fréquence et en temps. Des approches pour la détection qui s'intègrent bien avec ces exigences relatives à l'évaluation des paramètres, sans toutefois trop sacrifier la vitesse de traitement et la performance, seront bien plus désirables.

Comparé à la performance parfaite livrée par la méthode de maximum de vraisemblance, les approches utilisant le périodogramme ou la transformée de Fourier rapide à fréquence adaptée et lissée ont encore bien du chemin à parcourir. Il peut être aussi possible d'évaluer les profils en amplitude et en fréquence des bonds, à partir de

leur détection initiale, pour ensuite incorporer cette information dans le processus de détection afin d'en améliorer la performance. Comme solution de rechange, des méthodes statistiques d'ordre supérieur peuvent aussi être incorporées dans le processus pour profiter des propriétés statistiques d'ordre supérieur des signaux artificiels. Dans tous les cas, davantage de recherches doivent être excercée dans ce domaine pour étudier et/ou développer des approches, qui pourront fournir des performances de détection améliorées pour des utilisations pratiques.

Read, W.J.L. 2002. Detection of frequency hopping signals in digital wideband data. DRDC Ottawa TR 2002-162. R&D pour la défense Canada – Ottawa.

Table of contents

List of figures

List of tables

This page intentionally left blank.

1. Introduction

The introduction of wideband receivers to modern Communications Electronics Support Measures systems, as well as the ongoing technological advances in computer systems, have made it possible to apply better and better approaches to the problem of signal detection and estimation. Of particular interest is the detection and estimation of the short duration signals (hops) generated by frequency hopping radios, which have begun to proliferate on the modern battlefield.

Frequency hopping radios broadcast a signal by transmitting the signal for a short period of time (generally less than 100 ms), then retuning the signal to a new frequency and repeating the process. Frequencies are chosen on a pseudo-random basis, typically number in the hundreds, and can cover a frequency band of tens of MHz or more. For the interceptor, it is a difficult problem since the pseudo-random sequence used to choose the hop frequency is usually unknown, so the signal cannot be tracked using a fast-retuning narrowband receiver.

With wideband receivers, it is possible to capture and record every hop transmitted by a frequency hopping radio, assuming that the receiver has a bandwidth equal to or larger than the hop band, and that the receiver is covering the right portion of the frequency spectrum. In this case, the problem is that the receiver also records all the other noise and signals that are present in the frequency band. This makes it much more difficult to find and track the targeted hopping signal, especially when these other signals are stronger.

In this report, methods of detecting short duration signals in digital wideband receiver data are assessed and compared. The assessment starts in Section 2 by considering the performance of an idealized detector, and using this as a basis for a performance comparison. A number of methods are then introduced in Sections 3 and 4, and analyzed extensively in terms of determining detection performance. Implementation issues which affect detection performance or inband interference (from other signals) are also explored. This is followed by some comparisons of detection performance through Monte Carlo simulations and a comparison of processing times in Section 5. Concluding remarks are provided in Section 6.

2. Ultimate Detection Limit

The ability to detect short duration frequency hopped signals in digital wideband data corrupted by noise will be influenced by the *a priori* information that is available, and how this information is used. In the ideal case, the complex baseband envelope of the signal will be known exactly and only the hop start time, center frequency, and power will be unknown. The ideal case is unlikely to be realized in practical situations since the modulation content of a signal will normally be unknown. However, analyzing the ideal case yields a useful standard by which other methods may be compared and evaluated.

The approach used here is to first develop the maximum likelihood method for detection of a single hop in noise. As will be seen, this leads to an approach which involves searching for peaks in a time/frequency correlation spectrum. In practical spectral search techniques, a detection threshold is used to determine whether a peak is due to a signal or noise. Using this idea, a statistical analysis is performed to determine the false detection or false alarm rate as a function of the threshold setting, and also to determine the successful detection rate as a function of both the threshold setting and the signal-to-noise ratio (SNR).

In developing a maximum likelihood detection approach for a hop signal in noise, the first step is to define the data model. For wideband baseband data containing a single hop in noise, the model can be expressed as

$$x(n) = as(n - t_o)e^{j2\pi f_c n} + \sigma\nu(n) \qquad \text{for} \quad n = 0, 1, ..., N-1 \tag{1}$$

where the following definitions are used:

N	number of samples of wideband data
M	length of hop in terms of the number of data samples
t_o	hop start time index (i.e. the hop starts at $n = t_o$)
f_c	hop center frequency normalized with respect to the sampling frequency f_s (i.e. $0 \leq f_c < 1$)
σ	real-valued noise amplitude
$\nu(n)$	complex noise normalized so that $E\{\|\nu(n)\|^2\} = 1$
a	complex-valued signal amplitude
$s(m)$	complex baseband signal envelope for $0 \leq m < M$ (i.e. during hop) and $s(m) = 0$ for all other values of m. Also normalized so that $E\{\|s(m)\|^2\} = 1$.

In the ideal case being considered, the values of a, t_o, f_c, and σ are all assumed to be unknown.

Given that the noise is white Gaussian in nature, the hop start time and center frequency

can be estimated by minimizing the least squares error[1] given by

$$\epsilon^2 = \sum_{n=0}^{N-1} |x(n) - \hat{a}s(n - \hat{t_o})e^{j2\pi\hat{f}_c n}\ |^2 \tag{2}$$

where $\hat{a}$, $\hat{t_o}$ and $\hat{f}_c$ are the estimated quantities of interest. There is no known closed form solution for this expression, however by minimizing ϵ^2 with respect to $\hat{a}$, and assuming that the data contains the entire hop (i.e. $M + t_o \leq N$), then $\hat{a}$ may be eliminated and the following simplified expression obtained:

$$S(t, f) = \sum_{n=0}^{N-1} x(n)s^*(n - t)e^{-j2\pi fn} \tag{3}$$

where the optimum values of $(t, f) = (\hat{t_o}, \hat{f}_c)$ are those which maximize $|S(t, f)|$. The form of this expression may be interpreted as the Fourier transform of the sequence represented by $x(n)s^*(n - t)$ for $n = t, ..., t + M - 1$. Taking advantage of Fourier transform theory, the natural choices for the frequency values are $f = 0, 1/M, 2/M, ..., (M - 1)/M$.

To illustrate the result of using $S(t, f)$, a simulated sample of wideband data ($N = 500$) was generated containing a single hop signal ($M = 100$) in white Gaussian noise. The hop signal was defined so that $s(n - t_o) = 1$ for $t_o \leq n < t_o + M$, and $s(n - t_o) = 0$ otherwise, as shown in Figure 1a. The start time and center frequency parameters were chosen to be $(t_o, f_c) = (200, 0.5)$. Defining the input signal-to-noise power ratio as

$$\mathit{snr} = \frac{|a|^2}{\sigma^2} \tag{4}$$

the noise level was set so that $10 \log \mathit{snr} = 0$ dB. The amplitude of the hop signal plus noise is shown in Figure 1b.

Using a time-frequency search strategy, the results of using $|S(t, f)|$ are plotted in Figure 2a. Figure 2b and 2c show cross sections of the time and frequency profiles, respectively. The width of the peaks are related to the inverse of the hop bandwidth (time profile) and inverse of the hop time duration (frequency profile). In the example, the small hop bandwidth of $1/M$ (for the duration of the hop, the bandwidth was zero however the truncated nature of the signal widens the overall bandwidth) results in a peak in the time profile with a width at the base of $\Delta t = 2M = 200$. Visually, the peak in the frequency profile appears considerably narrower and its width is given by $\Delta f = 2/M = 0.02$.

[1] For signals in additive white Gaussian noise, the least squares estimate is equivalent to the maximum likelihood estimate.

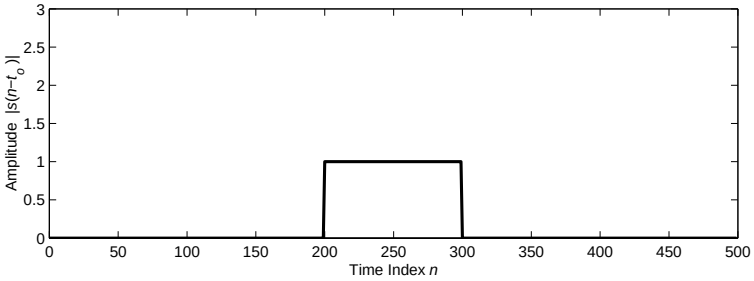

(a)

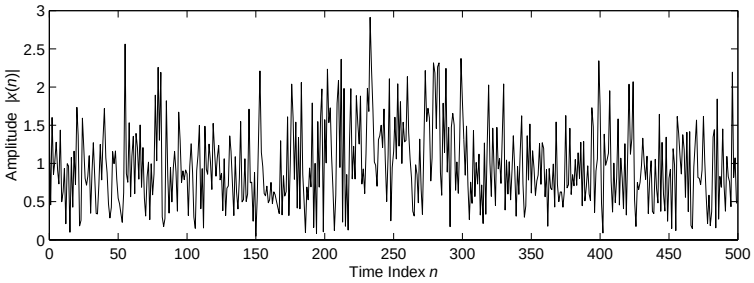

(b)

Figure 1: *Hop signal amplitude as a function of time for (a) the noiseless case, and (b) for* $10 \log snr = 0$ *dB.*

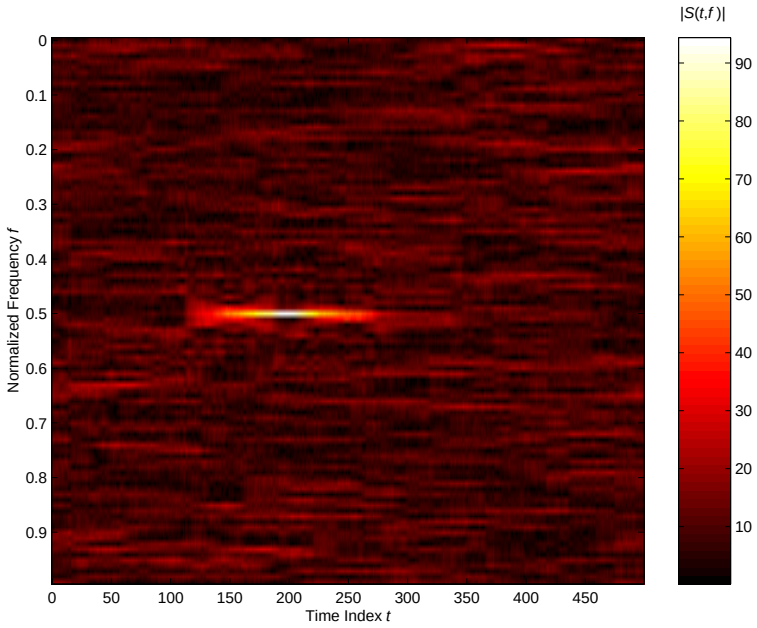

(a)

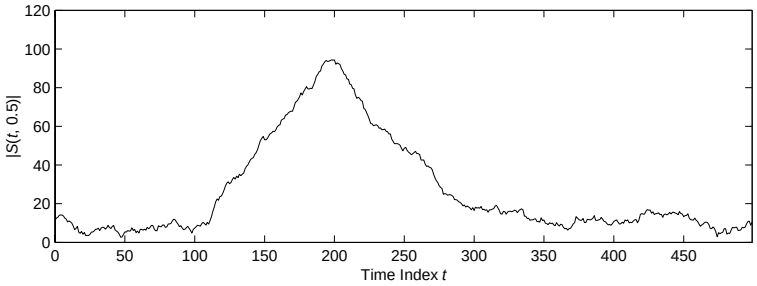

(b)

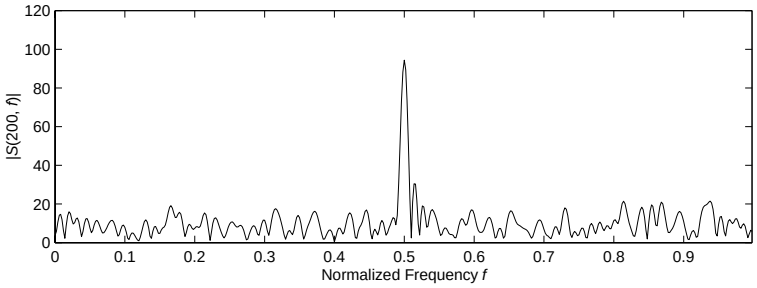

(c)

Figure 2: *Maximum likelihood search results showing (a) the time-frequency spectrum $|S(t,f)|$, (b) the time profile for $f = 0.5$, and (c) the frequency profile for $t = 200$.*

2.1 Probability of False Alarm

For practical applications, and since it will not necessarily be known whether a sample of data actually contains any hop signals, it is useful to define a threshold. Any peak in $S(t, f)$ exceeding this threshold is considered a detection, otherwise it is ignored as being generated by noise effects. The level of the threshold is chosen high enough that noise generated peaks infrequently exceed the threshold, but not so high that signal generated peaks fall below the threshold and do not get detected. In this section, the problem of false detections is considered.

To begin the analysis, the data model for $x(n)$ given in (3) is expanded using the signal plus noise definition given in (1), and the case where $(t, f) \neq (t_o, f_c)$ is considered. Expanding (3) as discussed, then

$$\begin{aligned} S(t,f) &= \sum_{n=0}^{N-1} (as(n-t_o)e^{j2\pi f_c n} + \sigma\nu(n))s^*(n-t)e^{-j2\pi fn} \\ &= \sum_{n=0}^{N-1} \left[as(n-t_o)s^*(n-t)e^{j2\pi(f_c-f)n} + \sigma\nu(n)s^*(n-t)e^{-j2\pi fn}\right] \\ &= a\sum_{n=0}^{N-1} s(n-t_o)s^*(n-t)e^{j2\pi(f_c-f)n} + \sigma \sum_{n=t}^{t+M-1} \nu(n)s^*(n-t)e^{-j2\pi fn} \end{aligned} \tag{5}$$

The first summation term goes to zero if there is no overlap between the actual hop $s(n - t_o)$ and the predicted hop $s(n - t)$. If there is some overlap, then $s(n - t_o)s^*(n - t)$ can be represented by a process with constant amplitude but random phase. Using the central limit theorem [1], the result of the summation will be

$$\sum_{n=0}^{N-1} s(n-t_o)s^*(n-t)e^{j2\pi(f_c-f)n} = \sqrt{M-|t-t_o|}\nu_1 \tag{6}$$

where ν_1 is complex zero-mean Gaussian variable with a variance of one. The second term can be replaced by $\sigma\sqrt{M}\nu_2$ (where ν_2 has the same statistical properties as ν_1) since $s^*(n - t)e^{-j2\pi fn}$ has no statistical effect and the sum of N zero-mean Gaussian random variables with variances of σ^2 yields a new zero-mean Gaussian random variable with a variance $M\sigma^2$ [1]. Hence (5) becomes

$$S(t,f) = a\sqrt{M-|t-t_o|}\nu_1 + \sigma\sqrt{M}\nu_2 \tag{7}$$

Generally, the worst case occurs when $t \approx t_o$, which maximizes the effect of the interference term $s(n-t_o)s^*(n-t)$ in (6), and ultimately maximizes the size of undesired peaks in $|S(t,f)|$ (where the undesired peaks are those which do not contain the time-frequency point (t_o, f_c)).

To simplify the notation, the definition $K = M - |t - t_o|$ where $0 \leq K \leq M$ is used to get

$$S(t,f) = a\sqrt{K}\nu_1 + \sigma\sqrt{M}\nu_2 \tag{8}$$

with the first and second order statistics given by

$$E\{S(t,f)\} = 0 \tag{9}$$

and

$$VAR\{S(t,f)\} \;=\; |a|^2 K \;+\; \sigma^2 M \;=\; \sigma_2^2 \tag{10}$$

The corresponding probability density function, with respect to the random amplitude variable, $r = |S(t,f)|$, and the random phase variable, $\theta = \angle S(t,f)$, is given by

$$f_{R\Theta}(r,\theta) = \frac{r}{\pi\sigma_2^2} e^{-r^2/\sigma_2^2} \tag{11}$$

A false detection occurs when $r > \tau\sigma\sqrt{M}$ where τ is the amplitude threshold level defined relative to the base noise floor of $S(t,f)$ (i.e. the standard deviation of the noise level when no hop signals are present). The probability of false alarm, *for a given choice of* (t,f), is given by

$$\begin{aligned} P(r > \tau\sigma\sqrt{M} \mid t,f) &= \int_{\tau\sigma\sqrt{M}}^{\infty} \int_0^{2\pi} f_{R\Theta}(r,\theta)\, d\theta dr \\ &= \int_{\tau\sigma\sqrt{M}}^{\infty} \int_0^{2\pi} \frac{r}{\pi\sigma_2^2} e^{-r^2/\sigma_2^2}\, d\theta dr \\ &= e^{-M\tau^2\sigma^2/\sigma_2^2} \\ &= e^{-M\tau^2/(K\mathit{snr}+M)} \end{aligned} \tag{12}$$

It is useful to define the two limiting cases as

$$PF_1 \;=\; e^{-\tau^2} \tag{13}$$

$$PF_2 \;=\; e^{-\tau^2/(\mathit{snr}+1)} \tag{14}$$

where PF_1 represents the case where there is no hop signal in the interval $x(t), ..., x(t+M-1)$ (noise only) and PF_2 represents the case where a hop signal occupies the entire interval (signal interference).

A fortunate feature of the signal interference peaks in the time/frequency spectrum is that they will always be smaller than the associated signal peak. Hence, in data sets with only a single hop occurring at a time (which is the assumption that has been made for the ideal case), the signal peak can easily be identified and the associated interference peaks ignored. The probability of false alarm is therefore given by (13).

In practical real-world situations, data sets with two or more hops overlapping in time (but separated in frequency) are possible, so that interference effects cannot be ignored as in the ideal single hop case. Detection methods designed to handle multiple hop data sets (e.g. see Sections 3 and 4) manifest interference as sidelobe effects, which can be treated as a separate issue (i.e. inband interference). Hence, the definition of the probability of false alarm is also restricted to the noise-only case throughout the rest of this report.

Having restricted the definition of the probability of false alarm to PF_1, a few comments are in order. The first is that the probability of false alarm drops rapidly as the threshold increases above the noise floor, as shown in Figure 3. If a specific probability of false alarm is desired, then the threshold τ can be calculated by rearranging (13) to get

$$\tau \quad = \quad \sqrt{-\ln(PF_1)} \tag{15}$$

An obvious advantage of the definition used here for the threshold (i.e. defined relative to the spectral noise floor), is that for a fixed probability of false alarm, τ is independent of M or N.

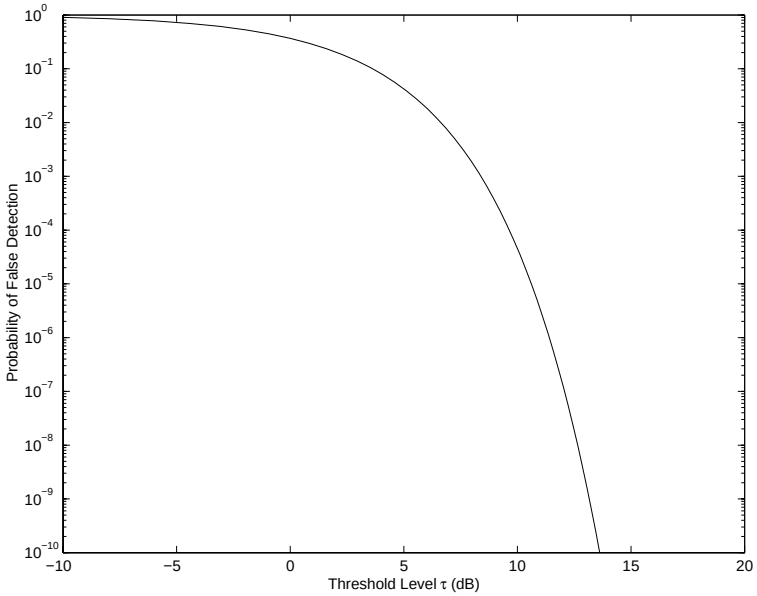

Figure 3: *The probability of false alarm as a function of the threshold (measured in dB)*

Another comment is that the probability of false alarm may be used to determine the expected number of false detections for all $N \times M$ possible choices of (t, f). Ideally,

this would simply be a case of adding the individual probabilities. However, there are underlying correlations in $S(t, f)$ which must be accounted for. Since $S(t, f)$ is generated from N input samples, the effective number of uncorrelated values of $S(t, f)$ should also be N. To show this, consider that (3) may be regarded as an expression for an M-tap filter when $f = f_1$ is fixed, and regarded as a Fourier transform when $t = t_1$ is fixed. For a fixed value of $f = f_1$, the outputs $S(t_1, f_1)$ and $S(t_2, f_1)$ will be uncorrelated only if $|t_1 - t_2| \geq M$. Hence, for N choices of t, there are effectively only N/M uncorrelated output samples available. For a fixed value of the time index $t = t_1$, there are M choices of f leading to M uncorrelated output samples (from Fourier transform theory). Thus, for all values of $S(t, f)$, there are effectively $N/M \times M = N$ uncorrelated output samples available.

A final comment is that for a given input sample size, the expected number of false detections is given by

$$\textit{Expected Number of False Detections} \quad = \quad NPF_1 \quad = \quad Ne^{-\tau^2} \tag{16}$$

2.2 The Probability of Detection

For detection of a hop signal to occur, the corresponding peak generated in the time/frequency spectrum, $S(t, f)$, must exceed a predefined threshold. The analysis of the probability of this occurring begins with the expansion of (3) using (1), for the case when $(t, f) = (t_o, f_c)$. This yields

$$\begin{aligned} S(t_o, f_c) &= \sum_{n=0}^{N-1} (as(n - t_o)e^{j2\pi f_c n} + \sigma\nu(n))s^*(n - t_o)e^{-j2\pi f_c n} \\ &= \sum_{n=0}^{N-1} \left[a|s(n - t_o)|^2 + \sigma\nu(n)s^*(n - t_o)e^{-j2\pi f_c n}\right] \\ &= aM + \sum_{n=t_o}^{t_o+M-1} \sigma\nu(n)s^*(n - t_o)e^{-j2\pi f_c n} \end{aligned} \tag{17}$$

To simplify the derivation, $s(m)$ is assumed to be a constant modulus signal (i.e. $|s(m)| = 1$). Using the constant modulus assumption, the term $\nu(n)s^*(n - t_o)e^{-j2\pi f_c n}$ can be replaced by the equivalent Gaussian noise sequence $\nu'(n)$ with the same statistical properties, hence

$$\begin{aligned} S(t_o, f_c) &= aM + \sum_{n=t_o}^{t_o+M-1} \sigma\nu'(n) \\ &= aM + \sigma\sqrt{M}\nu_3 \end{aligned} \tag{18}$$

where ν_3 is a complex zero-mean Gaussian random variable with a variance of one, and the term $\sigma\sqrt{M}\nu_3$ is the result of the sum of N zero-mean Gaussian random variables.

The first and second order statistical results for (18) are therefore

$$E\{S(t_o, f_c)\} = aM \tag{19}$$

and

$$VAR\{S(t_o, f_c)\} = \sigma^2 M \tag{20}$$

The results for other modulations will not be appreciably different. For example, if $s(m)$ can be represented as a Gaussian process, the result of $\nu(n)s^*(n - t_o)$ is a new process which is approximately Gaussian with the same first and second order statistics as $\nu(n)$. The results for (19) and (20) will then be the same.

Given the mean and variance of $S(t_o, f_c)$, the probability density function can be written in terms of the random amplitude variable, $r = |S(t_o, f_c)|$, and random phase variable, $\theta = \angle S(t_o, f_c)$, as

$$f_{R\Theta}(r, \theta) = \frac{r}{\pi\sigma^2 M} e^{-(r^2 - 2r|a|M\cos\theta + |a|^2M^2)/\sigma^2 M} \tag{21}$$

A successful detection occurs when the hop signal peak exceeds the threshold, or $r > \tau\sigma\sqrt{M}$. The probability of a successful detection is therefore

$$\begin{aligned} P(r_1 > \tau\sigma\sqrt{M}) &= \int_{\tau\sigma\sqrt{M}}^{\infty}\int_0^{2\pi} f_{R\Theta}(r, \theta)d\theta dr \\ &= \int_{\tau\sigma\sqrt{M}}^{\infty}\int_0^{2\pi} \frac{r}{\pi\sigma^2 M} e^{-(r^2 - 2r|a|M\cos\theta + |a|^2M^2)/\sigma^2 M} d\theta dr \\ &= \int_{\tau\sigma\sqrt{M}}^{\infty} \frac{2r}{\sigma^2 M} e^{-(r^2 + |a|^2M^2)/\sigma^2 M} I_o(2r|a|/\sigma^2)dr \end{aligned} \tag{22}$$

where $I_o()$ is the modified Bessel function of the first kind and of order zero. There is no simple solution for this integral, but a useful series approximation [2] is given by

$$\begin{aligned} P(r_1 > \tau\sigma\sqrt{M}) &= \frac{1}{2}\left(1 - \text{erf}\left(\frac{(\tau\sigma - |a|\sqrt{M})}{\sigma}\right)\right) + \frac{\sigma}{4|a|\sqrt{M\pi}} e^{-(\tau\sigma - |a|\sqrt{M})^2/\sigma^2} \\ &\quad \times \left(1 - \frac{\tau\sigma - |a|\sqrt{M}}{4|a|\sqrt{M}} + \frac{\sigma^2 + 2(\tau\sigma - \sqrt{M}|a|)^2}{16|a|^2 M} - ...\right) \end{aligned} \tag{23}$$

Using the definition for *snr* in (4), the final form of the probability of detection can be written as

$$PD \approx \frac{1}{2}\left(1 - \text{erf}(\alpha)\right) + \frac{1}{4\sqrt{\pi M snr}} e^{-\alpha^2}\left(1 - \frac{\alpha}{4\sqrt{M snr}} + \frac{1 + 2\alpha^2}{16 M snr}\right) \tag{24}$$

where

$$\alpha = \tau - \sqrt{M snr} \tag{25}$$

Some curves representing the probability of detection as a function of SNR, calculated using (24), are plotted in Figure 4. For these curves, various values of the threshold τ were considered. Inspecting (24) and (25), if M*snr* remain constant, then the probability of detection will also remain constant. Hence the parameters M and *snr* are inversely related for a constant probability of detection. Using this fact, the value of the SNR (in dB) can be conveniently represented by the values shown on the X-axis of the plot in Figure 4 minus $10 \log M$. Note that below 0 dB, the values of the curve for $\tau = 5$ dB are inaccurate (too high) due to approximation error in (24).

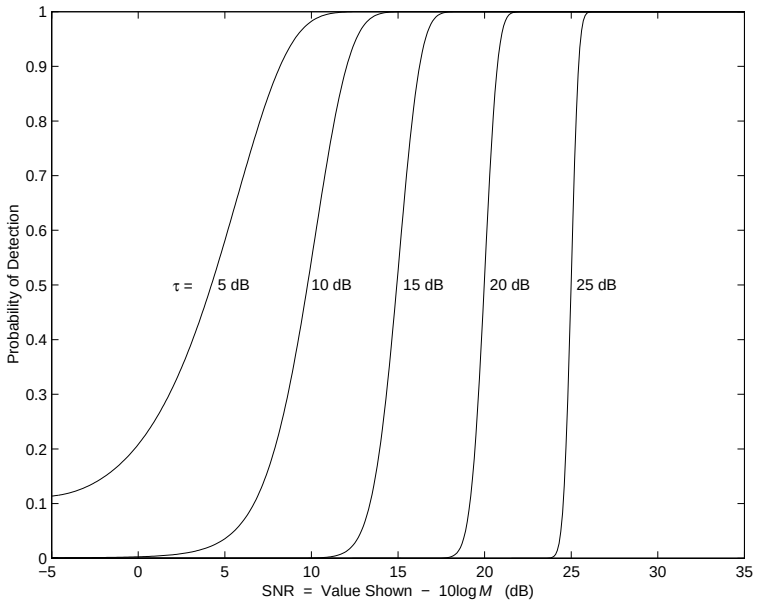

Figure 4: *The probability of detection as a function of SNR for various threshold settings*

The results in Figure 4 may be combined with the results in Figure 3 to determine detection performance under various conditions. For example, consider the case where the desired probability of false alarm (PF_1) is 0.0001, the desired probability of detection is 0.9, and the hop duration is $M = 1000$. From Figure 3 the desired threshold τ is 9.64 dB. Interpolating between $\tau = 5$ dB and $\tau = 10$ dB in Figure 4, for $PD = 0.9$ the X-axis value is 11.7 dB. Taking into account the effect of M, then the SNR is $11.7 - 30 = -18.3$ dB.

Clearly, as the hop duration increases, the same probability of detection can be achieved with a lower SNR. This can be conveniently represented as an effective processing gain of

$$\textit{Processing Gain} = 10 \log(M) \text{ dB} \tag{26}$$

The advantage of defining the effective processing gain is that it provides a useful method by which detection methods can be easily compared, rather than making comparisons using the equations for probability of false alarm and probability of detection (although the derivation of these probabilities is useful for determining the effective processing gain).

3. Hop Detection using a Channelizer

A very natural approach to processing wideband receiver data is to separate the data into N contiguous frequency channels covering the full input band. A major advantage is that since the bandwidth of most modern communications signals[2] is relatively narrow (< 1 MHz) compared to the receiver bandwidth, processing individual signals typically involves only a few frequency channels. Given that the sampling rate per channel can be reduced as much as F_s/N, the computational requirements for processing a single signal are dramatically reduced compared to processing the entire frequency band. A second advantage is that the SNR within a frequency channel is improved by $10 \log N$ dB since the noise is divided up over the N channels.

In terms of detecting frequency hopped signals in the presence of noise, the channelizing approach obviously has certain benefits due to the SNR improvement. However, unlike the maximum likelihood approach developed in Section 2, the hop signal envelope is assumed to be unknown. Typically the only information used is the hop bandwidth in order to select the most appropriate channel bandwidth. How this impacts detection performance is discussed in the next two sections (Sections 3.1 and 3.2) which deal with the FFT channelizer and the polyphase FFT channelizer, respectively. Another effect, which was briefly considered, is the effect of interference from other inband signals. For the real world, this is a common problem which will likely effect the choice of the channelizing technique. This will also be discussed.

3.1 FFT

For realtime processing, the FFT is a simple and attractive choice. Mathematically, the channelized output values can be represented by

$$y_k(t) = \sum_{n=0}^{N-1} w(n)x(n+t)e^{-j2\pi kn/N} \quad \text{for} \quad t = 0, N_b, 2N_b, ... \tag{27}$$

where N represents the number of samples in each FFT block and is usually chosen so that $N = 2^i$ and i is a positive integer (although variants exist which allow more flexibility in the choice of N), N_b represents the block shift (see Figure 5), $w(n)$ is the windowing function coefficient, $k = 0, 1, ..., N-1$ represents the frequency channel number, and the center frequency of each channel is given by k/N. Typically the FFT block size will be considerably shorter than the hop duration ($N \ll M$), so assuming a hop signal is present, each sample block will only represent a N/M slice of the hop. The choice of windowing function, represented by $w(n)$, is generally based on reducing the sidelobe level (where high sidelobes lead to interference problems from other inband signals) at the expense of frequency resolution (making it more difficult to resolve signals that are close in frequency). A good discussion of windowing functions for the Fourier transform is given in [3].

[2] PCS signals are ignored here since specialized receivers/approaches are required and this is outside the context of this report

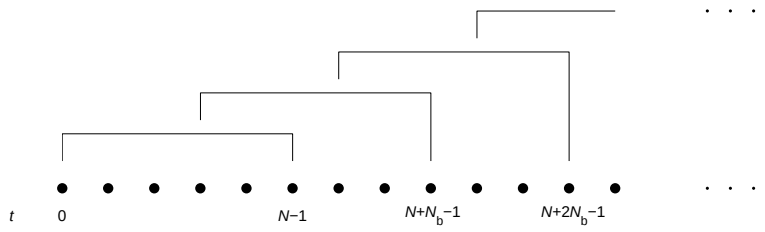

Figure 5: *Block shift processing scheme used for channelizing the data. The diagram shows the data (represented by the large dots) divided into overlapping blocks of length N with a shift value of N_b.*

Detection of hop signals involves finding the values of k where $|y_k(t)|$ exceeds a given threshold. This is repeated for each sample block. Although combining values of $y_k(t)$ from successive blocks could be used to improve the results, this kind of processing is not considered until Section 4. Here, only the results from single sample blocks are examined. Hence the notation can be simplified to

$$y_k = \sum_{n=0}^{N-1} w(n)x(n)e^{-j2\pi kn/N} \tag{28}$$

(where the "t" has been dropped) since in the statistical development that follows, the results for each sample block of data will be the same.

The hop signal plus noise model was presented in (1). To take into account the bandlimited nature of a real signal, a modified representation is used which shows the fundamental frequency components of the hop signal explicitly. It is given by

$$x(n) = \sum_{k=0}^{N-1} a_k e^{j2\pi kn/N} + \sigma\nu(n) \tag{29}$$

where $a_k = 0$ when $f = k/N$ is outside the frequency band of the signal, and $\sum_{k=0}^{N-1} |a_k|^2 = |a|^2$. Using this representation, (28) can be modified as follows:

$$\begin{aligned} y_k &= \sum_{n=0}^{N-1} w(n) \left(\sum_{m=0}^{N-1} a_m e^{j2\pi mn/N} + \sigma\nu(n) \right) e^{-j2\pi kn/N} \\ &= \sum_{n=0}^{N-1} w(n) \left(\sum_{m=0}^{N-1} a_m e^{j2\pi mn/N} \right) e^{-j2\pi kn/N} \\ &\quad + \sigma \sum_{n=0}^{N-1} w(n)\nu(n)e^{-j2\pi kn/N} \end{aligned} \tag{30}$$

The first term in the expression for y_k represents the Fourier transform calculation for the k^{th} coefficient, which is given by Na_k for a rectangular window. For any other

chosen windowing function, the result will be

$$\sum_{n=0}^{N-1} w(n) \left(\sum_{m=0}^{N-1} a_m e^{j2\pi mn/N} \right) = b_k \sum_{n=0}^{N-1} w(n) \tag{31}$$

where $b_k \approx a_k$ if a standard windowing function is used (i.e. one which tapers the data towards the end points and thus only slightly modifies the frequency content of the data). Noting also that the second term is essentially still noise, then the expression for y_k can be simplified to

$$\begin{aligned} y_k &= b_k \sum_{n=0}^{N-1} w(n) + \sigma \nu_k \sqrt{\sum_{n=0}^{N-1} w(n)^2} \\ &= b_k \beta_1 + \sigma \nu_k \beta_2 \end{aligned} \tag{32}$$

where ν_k is a zero-mean Gaussian random variable with unit variance representing the channel noise, and

$$\beta_1 = \sum_{n=0}^{N-1} w(n) \tag{33}$$

$$\beta_2 = \sqrt{\sum_{n=0}^{N-1} w(n)^2} \tag{34}$$

There are now two cases to be considered. The first is the case where the hop signal is completely contained in a single frequency channel. The second is the case where the hop signal spans two or more frequency channels, such as when the signal bandwidth exceeds the channel bandwidth. These two cases are discussed separately in sections Sections 3.1.1 and 3.1.2, which follow.

3.1.1 Single Channel Detection

The search spectrum for the single channel case can be defined as

$$S_{FFT_1}(f) = \sum_{n=0}^{N-1} w(n) x(n) e^{-j2\pi fn} \tag{35}$$

which is simply the definition for y_k except that the frequency, given by $f = k/N$ for $k = 0, ..., N-1$, is shown explicitly. The objective is to find the peaks in the frequency spectrum $|S_{FFT}(f)|$ which exceed a predefined threshold. The lack of a time parameter t reflects the fact that the processing for each block of data is the same (i.e. there is no time optimization).

In terms of the signal model, the signal frequency coefficients become

$$a_k = \begin{cases} a & \text{if} \quad k = Nf_c \\ \\ 0 & \text{if} \quad k \neq Nf_c \end{cases} \tag{36}$$

and the channel output values will then be

$$y_k = \begin{cases} \hat{a}\beta_1 + \sigma\beta_2\nu_k & \text{if} \quad k = Nf_c \\ \\ \sigma\beta_2\nu_k & \text{if} \quad k \neq Nf_c \end{cases} \tag{37}$$

where $b_k = \hat{a}$ for $k = Nf_c$. This result is similar to expressions developed for the maximum likelihood detector (see (8) and (18)) for the case where $M = N$ and $K = 0$. Hence, the same line of development is followed except with the following modifications to the spectral noise values

$$E\{S(f)\} = 0 \tag{38}$$

and

$$VAR\{S(f)\} = \sigma^2\beta_2^2 \tag{39}$$

where $f \neq f_c$, and the following modifications to the spectral signal peak

$$E\{S(f_c)\} = \hat{a}\beta_1 \tag{40}$$

and

$$VAR\{S(f_c)\} = \sigma^2\beta_2^2 \tag{41}$$

The probability of false alarm is therefore given by

$$PF_{FFT_1} \quad = \quad e^{-\tau^2} \tag{42}$$

As before, the threshold τ is a relative amplitude level defined with respect to the spectral noise floor; the absolute threshold is given by $\tau\sigma\beta_2$. The expected number of failures for an input set of N samples is NPF_{FFT_1}, when no signals are present in the data.

The probability of detection also follows as

$$PD_{FFT_1} \quad = \quad \frac{1}{2}\left(1 - \text{erf}(\alpha)\right) + \frac{1}{4\sqrt{\pi\beta snr}}e^{-\alpha^2}\left(1 - \frac{\alpha}{4\sqrt{\beta snr}} + \frac{1+2\alpha^2}{16\beta snr} - ...\right) \tag{43}$$

where

$$\beta \quad = \quad \frac{\beta_1^2}{\beta_2^2} \quad = \quad \frac{(\sum_{n=0}^{N-1} w(n))^2}{\sum_{n=0}^{N-1} w(n)^2} \tag{44}$$

and

$$\alpha \;=\; \tau - \sqrt{\beta snr} \tag{45}$$

The definition for β is useful as it represents the effective correlation time constant for the given windowing function[3], and $1/\beta$ is the effective noise bandwidth. Hence, when the rectangular window is used, $\beta = N$ and the false alarm and detection probabilities are identical to (14) and (24), respectively, for the case when $M = N$. For other common windowing functions (such as Hamming, Hanning, triangular, Blackman, Blackman-Harris, etc.), the correlation time constant β typically ranges between $0.5N$ and $0.75N$.

Noting that the term M in (24) and (25) has been replaced by β in (44) and (45), the processing gain expression in (26) can be adapted to become

$$\textit{Processing Gain} \;=\; 10\log\beta \;\text{ dB} \tag{46}$$

Although similar in form to the processing gain expression for the maximum likelihood detector, it falls short for several reasons. The first reason is that for any windowing function other than the rectangular window, $\beta < N$, so that windowing incurs a penalty of $10\log\beta/N$. The second reason is that since the FFT blocksize is normally chosen to be small enough to detect the shortest duration signals of interest, then generally $N < M$, and a further penalty of $10\log N/M$ is incurred. The last reason is that the estimation of the signal amplitude, $\hat{a}$, is influenced by the center frequency of the signal relative to the frequency channel and the bandwidth (greater signal bandwidth also reduces the magnitude of $\hat{a}$). The frequency offset problem is illustrated in Figure 6 which shows the filter response of the FFT (rectangular window) over seven consecutive frequency channels compared to the ideal channel filter response. In this case, as the frequency offset reaches half the channel bandwidth (-0.5 and 0.5), the reduction in $\hat{a}$ leads to a corresponding reduction in the processing gain of almost 4 dB.

Another problem with the FFT approach, which is also common to the maximum likelihood approach, is interference from inband signals. Specifically, the non-zero filter gain in the adjacent channels of the FFT response (high sidelobes) as shown in Figure 6 means that signals in these channels will have an affect on the target channel. Windowing functions such as Blackman-Harris can be used to suppress these sidelobes as shown in Figure 7, but the price is an increase in the channel bandwidth and a reduction in detection performance as already discussed.

[3]The effective correlation time constant of a filter is given by $\sum_{k=-\infty}^{\infty} R_{xx}(k)/R_{xx}(0)$ where $R_{xx}(k)$ represents the autocorrelation sequence of the filter [4]. Treating the windowing function values as filter coefficients, then $R_{xx}(-m) = \sum_{k=m}^{N-1} w(k)w(k-m)$ and $R_{xx}(m) = \sum_{k=0}^{N-m-1} w(k)w(k+m)$ for $m = 0, 1, ..., N-1$, and $R_{xx}(m) = 0$ for $|m| \geq N$. The result given in (44) then follows.

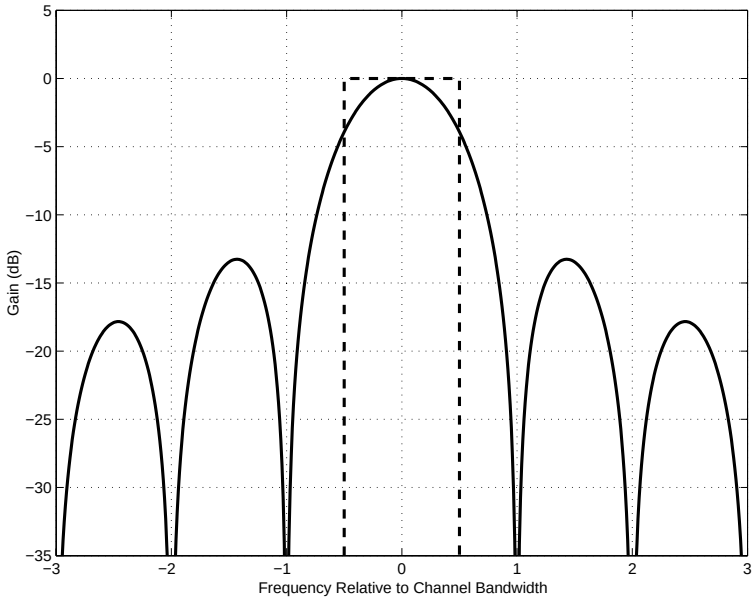

Figure 6: *Filter response of the FFT (solid line) for the target channel plus the three adjacent channels on either side. The ideal channel response is also shown (dashed line).*

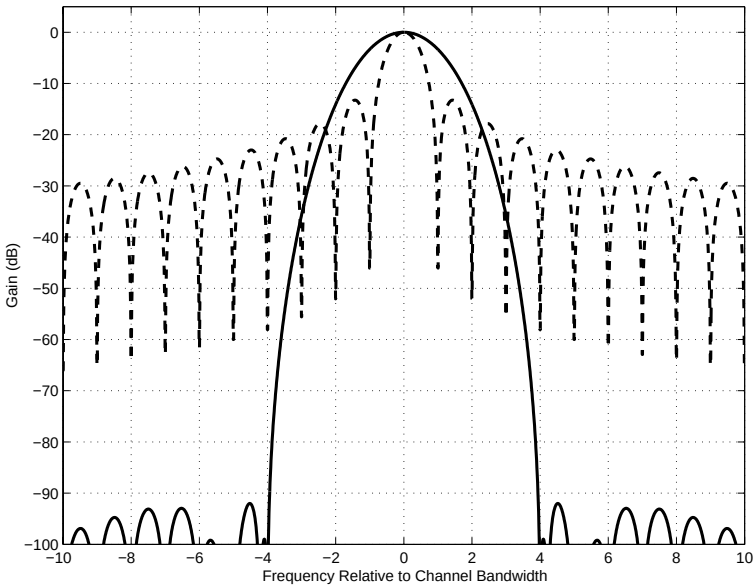

Figure 7: *Filter response of the FFT for the target channel plus the ten adjacent channels on either side using a Blackman-Harris window (solid line). The unwindowed response is also shown (dashed line) for comparison purposes.*

3.1.2 Frequency Smoothed Detection

In the case where the hop signal spans several frequency channels, and this span is known, then the channels may be combined according to

$$z_k = \sum_{n=k}^{k+L-1} \gamma_n y_n \tag{47}$$

where L is the number of channels spanned by the hop signal and γ_k is a weighting factor. Given that y_k represents the frequency spectrum (as estimated by the FFT), then z_k may be regarded as a smoothed frequency spectrum.

Since it is desirable to carry out the frequency smoothing in a way which enhances the SNR and, in turn, the detection performance, then the optimum choice for the weighting coefficients needs to be determined. To do this, the previous statistical result for y_k expressed in (32) can be easily modified for the channel spanning case giving

$$y_k = \begin{cases} b_k\beta_1 + \sigma\beta_2\nu_k & \text{if} \quad k = k_o, k_o+1, ..., k_o+L-1 \\ \\ \sigma\beta_2\nu_k & \text{if} \quad k = 0, 1, ..., k_o-1, k_o+L, ..., N-1 \end{cases} \tag{48}$$

where k_o is the lowest channel number of the frequency channels spanned by the hop signal. Incorporating this into (47) for $k = k_o$, the weighted output z_k becomes

$$z_{k_o} = \sum_{n=k_o}^{k_o+L-1} \gamma_n(b_n\beta_1 + \sigma\beta_2\nu_n) \tag{49}$$

By inspection, z_{k_o} consists of a signal term

$$s_o = \sum_{n=k_o}^{k_o+L-1} \gamma_n b_n \beta_1 \tag{50}$$

and a noise term

$$\eta_o = \sum_{n=k_o}^{k_o+L-1} \gamma_n \sigma\beta_2\nu_n \tag{51}$$

The optimum values of the weighting coefficients represented by γ_k will be the values that maximize the power difference between the signal term and the noise term. Since the expected power of the signal term is

$$E\{|s_o|^2\} \quad = \quad E\left\{ \left| \sum_{n=k_o}^{k_o+L-1} \gamma_n b_n \beta_1 \right|^2 \right\}$$

$$= \beta_1^2 \left| \sum_{n=k_o}^{k_o+L-1} \gamma_n b_n \right|^2 \tag{52}$$

and the expected power of the noise term is

$$E\{|\eta_k|^2\} = E\left\{ \left| \sum_{n=k_o}^{k_o+L-1} \gamma_n b_n \sigma \beta_2 \nu_n \right|^2 \right\}$$

$$= \sigma^2 \beta_2^2 \sum_{n=k_o}^{k_o+L-1} |\gamma_n|^2 \tag{53}$$

then maximizing the power difference is equivalent to maximizing

$$\frac{E\{|s_o|^2\}}{E\{|\eta_k|^2\}} = \frac{\beta \left| \sum_{n=k_o}^{k_o+L-1} \gamma_n b_n \right|^2}{\sigma^2 \sum_{n=k_o}^{k_o+L-1} |\gamma_n|^2} \tag{54}$$

where β was defined in (44). Taking the derivative of this expression with respect to γ_k and setting the result equal to zero yields

$$\gamma_k = \kappa b_k^* \tag{55}$$

where κ is an arbitrary constant. Incorporating these values back into the expression for the smoothed spectrum (47), the optimum result is given by

$$z_k = \sum_{n=k}^{k+L-1} \beta b_n^* y_n \tag{56}$$

where $\kappa = \beta$ was chosen for convenience. In practice, the actual value of b_n will be unknown, but since $E\{\beta b_n^* y_n\} = \beta^2 b_n^* b_n$ and $E\{y_n^* y_n\} = \beta^2 b_n^* b_n + \beta\sigma^2$, then an appropriate estimate of the smoothed spectrum is given by

$$\hat{z_k} = \sum_{n=k}^{k+L-1} (y_n^* y_n - \beta\sigma^2)$$

$$= -L\beta\sigma^2 + \sum_{n=k}^{k+L-1} y_n^* y_n \tag{57}$$

The detection equation can now be written as

$$S_{FFT_L}(f) = \sum_{n=k}^{k+L-1} y_n^* y_n \tag{58}$$

$$= \sum_{n=k}^{k+L-1} \left| \sum_{n=0}^{N-1} w(n)x(n)e^{-j2\pi kn/N} \right|^2 \quad (59)$$

where $f = k/N$ for $k = 0, 1, ..., N - L$. Note that the constant term $-L\beta\sigma^2$ has been dropped, since it has no effect on the maximization.

To determine either the probability of false alarm or the probability of detection, it is useful to first expand y_k in (58) in terms of its statistical representation given in (32) which yields

$$\begin{aligned} S_{FFT_L}(f) &= \sum_{n=k}^{k+L-1} (b_n\beta_1 + \sigma\beta_2\nu_n)(b_n\beta_1 + \sigma\beta_2\nu_n)^* \\ &= \sum_{n=k}^{k+L-1} \sigma^2\beta_2^2|\nu_n|^2 + |b_n|^2\beta_1^2 + 2\sigma\beta_1\beta_2 Re\{b_n\nu_n^*\} \end{aligned} \quad (60)$$

The three terms of this summation will now be used to develop the probability of false alarm and the probability of detection.

The Probability of False Alarm

The first summation term in (60) is a noise-only term given by

$$v = \sum_{n=k}^{k+L-1} \sigma^2\beta_2^2|\nu_n|^2 \quad (61)$$

The probability density function (pdf) of this noise term can be derived beginning with the pdf of the random amplitude variable, $r = |\nu_n|$, and random phase variable, $\theta = \angle\nu_n$, which is given by

$$f_{R\Theta}(r, \theta) = \frac{r}{\pi} e^{-r^2} \quad (62)$$

The marginal pdf obtained by integrating out θ is given by

$$f_R(r) = \int_o^{2\pi} f_{R\Theta}(r, \theta)d\theta = 2re^{-r^2} \quad (63)$$

Defining $u = \sigma^2\beta_2^2|\nu_n|^2 = \sigma^2\beta_2^2 r^2$, the pdf of v then follows from

$$\begin{aligned} f_U(u) &= f_R(r) \left| \frac{dr}{du} \right| \\ &= f_R(\sqrt{u/\sigma^2\beta_2^2}) \left| \frac{d\sqrt{u/\sigma^2\beta_2^2}}{du} \right| \\ &= \frac{1}{\sigma^2\beta_2^2} e^{-u/\sigma^2\beta_2^2} \end{aligned} \quad (64)$$

which is an exponential distribution. The solution for the summation of identically distributed independent exponential random variables is an m-Erlang random variable. Hence, the desired pdf is given by

$$f_V(v) = \frac{v^{L-1} e^{-v/\sigma^2\beta_2^2}}{\sigma^{2L}\beta_2^{2L}(L-1)!} \tag{65}$$

with

$$E\{v\} = L\sigma^2\beta_2^2 \tag{66}$$

and

$$VAR\{v\} = L\sigma^4\beta_2^4 \tag{67}$$

If the power threshold τ^2 is defined relative to the spectral noise floor (given by $E\{v\}$ in this case) then a false detection occurs when $v > \tau^2 L\sigma^2\beta_2^2$. Hence the probability of false alarm is given by

$$\begin{aligned} PF_{FFT_L} &= \int_{\tau^2 L\sigma^2\beta_2^2}^{\infty} f_V(v)\, dv \\ &= \int_{\tau^2 L\sigma^2\beta_2^2}^{\infty} \frac{v^{L-1} e^{-v/\sigma^2\beta_2^2}}{\sigma^{2L}\beta_2^{2L}(L-1)!}\, dv \\ &= e^{-\tau^2 L} \sum_{k=0}^{L-1} \frac{(\tau^2 L)^k}{k!} \end{aligned} \tag{68}$$

The Probability of Detection

The second summation term in (60) is a signal only term and exists only when a signal spans any of channels k to $k + L - 1$. It is a constant term which can be represented by

$$m = \beta_1^2 \sum_{n=k}^{k+L-1} |b_n|^2 \tag{69}$$

The third summation term in (60), represented by

$$w = 2\sigma\beta_1\beta_2 \sum_{n=k}^{k+L-1} Re\{b_n \nu_n^*\} \tag{70}$$

is due to cross-correlation between the signal and noise, and like the first term, exists only when there is signal present in any of channels k to $k + L - 1$. Inspecting this term, and given that σ, β_1, β_2, and b_n are constants, the cross-correlation term has a real-valued zero-mean Gaussian distribution with a variance given by $2\sigma^2\beta_1^2\beta_2^2|b_n|^2$ for a given value of n (where

$VAR\{Re\{\nu_n\}\} = \frac{1}{2}VAR\{\nu_n\}$ was used). The summation of L independent zero-mean Gaussian variables produces a new zero-mean Gaussian variable whose variance is the sum of the L individual variances. Therefore

$$E\{w\} = 0 \tag{71}$$

and

$$VAR\{w\} = 2\sigma^2\beta_1^2\beta_2^2 \sum_{n=k}^{k+L-1} |b_n|^2 \tag{72}$$

Defining the new random variable ψ as the sum of the three terms, then

$$\psi = v + w + m \tag{73}$$

The mean and variance of ψ is the sum of the individual means and variances already calculated for v, w, and m, thus

$$E\{\psi\} = L\sigma^2\beta_2^2 + \beta_1^2 \sum_{n=k}^{k+L-1} |b_n|^2 \;\; = \;\; \overline{\psi} \tag{74}$$

and

$$VAR\{\psi\} = L\sigma^4\beta_2^4 + 2\sigma^2\beta_1^2\beta_2^2 \sum_{n=k}^{k+L-1} |b_n|^2 \;\; = \;\; \gamma^2 \tag{75}$$

Unfortunately, the determination of the corresponding pdf leads to complications since v and w are random variables with different distributions. Hence, as a first approximation, ψ is assumed to have a Gaussian distribution with the mean and variance given in (74) and (75), respectively. The approximate pdf is given by

$$f_\Psi(\psi) \approx \frac{1}{\sqrt{2\pi}\gamma} e^{-(\psi-\overline{\psi})^2/2\gamma^2} \tag{76}$$

Using this approximate pdf, the probability of detection becomes

$$\begin{aligned} PD_{FFT_L} &= \int_{\tau^2 L\sigma^2\beta_2^2}^{\infty} f_\Psi(\psi)\, dw \\ &= \int_{\tau^2 L\sigma^2\beta_2^2}^{\infty} \frac{1}{\sqrt{2\pi}\gamma} e^{-(w-\overline{\psi})^2/2\gamma^2}\, dw \\ &= \frac{1}{2} + \frac{1}{2}\text{erf}\left(\frac{\overline{\psi} - \tau^2 L\sigma^2\beta_2^2}{\sqrt{2}\gamma}\right) \\ &= \frac{1}{2} + \frac{1}{2}\text{erf}\left(\frac{\beta snr + L(1-\tau^2)}{\sqrt{2L + 4\beta snr}}\right) \end{aligned} \tag{77}$$

where (4), (44), (74), and (75) were used, and where

$$|a|^2 \approx \sum_{n=k}^{k+L-1} |b_n|^2 \tag{78}$$

when frequency channels k to $k + L - 1$ completely contain the hop signal.

Since the expression for the probability of false alarm (68) is independent of N, and therefore so is τ, the probability of detection will remain constant as long as βsnr is constant. The same effect observed for the maximum likelihood and the single channel FFT detection approaches.

An advantage of using a channel bandwidth that is smaller than the signal bandwidth is that it leads to a better representation of the signal, since finer frequency sampling is being performed (relative to the signal bandwidth). This helps to overcome the problem of losses due to mismatches between the signal frequency and the channel center frequency, or due to modulation effects, experienced when using the single channel approach.

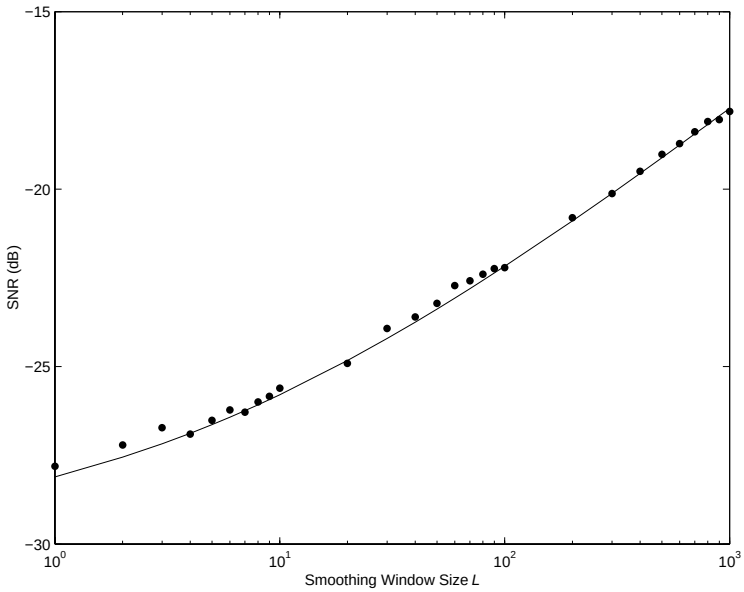

Figure 8: *Performance penalty incurred as a function of the frequency smoothing window size. The results were calculated for $N = 10000$ and show the SNR required to achieve a probability of detection of 0.9 when the threshold τ is set for a probability of false alarm of 0.0001. The dots show the SNR values determined through Monte Carlo simulations.*

Despite the apparent advantages, there is a penalty for frequency smoothing. Although not obvious from inspecting (68) and (77), the problem is illustrated in Figure 8. This figure shows the increase in SNR that is required to maintain the same probability of detection when the smoothing window size L is increased (the probability of false alarm is also kept fixed). Both theoretical

(solid line) and experimental (dots) results are shown. For the theoretical results, an SNR value was calculated for each value of L by first iteratively solving (68) to find the appropriate value of τ for the given probability of false alarm. Using this value, (77) was then solved directly to get the SNR for the desired probability of detection. The experimental results consisted of Monte Carlo computer simulations to iteratively determine the SNR values leading to the desired probability of detection, where the corresponding choices of τ were the same as used for the theoretical results. When adjusting the SNR values, 100 trials were used to estimate the probability of detection for each adjustment. The purpose of the experimental results was to verify the accuracy of the Gaussian approximation used when deriving (77). As can be seen, the agreement between the theoretical approximation and experimental results is very good.

One way to understand the relationship between the SNR and the smoothing window size illustrated in Figure 8 is to consider the spectral signal-to-noise power ratio defined by

$$\textit{Spectral}_{\textit{snr}} \;=\; \frac{E\{w+m\}}{\sqrt{VAR\{v\}}} \tag{79}$$

which provides a measure of how well the spectral peak can be distinguished from the noise peaks (note that the spectral peak is properly represented by $v+m+w$, however, for detection purposes, only the height of the peak above the noise floor is of interest). Using (66), (67), and (74), the spectral SNR is given by

$$\textit{Spectral}_{\textit{snr}} \;=\; \frac{|a|^2\beta_1^2}{\sqrt{L\sigma^4\beta_2^4}} = \;\frac{\textit{snr}\beta}{\sqrt{L}} \tag{80}$$

The effect of $\sqrt{L}$ in the denominator is to degrade detection performance as L increases. The corresponding processing gain is therefore

$$\textit{Processing Gain} \;\approx\; 10\log\beta - 5\log L \;\text{ dB} \tag{81}$$

Examining the expression for processing gain, a $-5\log L$ dB penalty is incurred by smoothing. Comparing this to Figure 8, the actual penalty is somewhat less for smaller window sizes (i.e. $L < 100$), but begins to exhibit behaviour which is consistent with the estimated penalty for larger values of L. A good approximation to the actual smoothing penalty is given by

$$\textit{Smoothing Penalty} = -5\log(L + 4L^{\frac{1}{2}} + 4) + 5\log 9 \quad \text{dB} \tag{82}$$

and after the appropriate modification the processing gain expression becomes

$$\textit{Processing Gain} \;=\; 10\log\beta - 5\log(L + 4L^{\frac{1}{2}} + 4) + 5\log 9 \;\text{ dB} \tag{83}$$

Earlier, L was defined as the number of frequency bins spanned by the signal. If the effect of sidelobes is included, and given that real-world filters used to bandlimit transmitted signals are not perfect brick-wall filters, there is no hard limit on the number of frequency channels that will be spanned by a signal. A more appropriate definition for L is to choose the value which maximizes the SNR (in dB) of the signal within the L channels plus the processing gain (in dB) given the signal definition in (29). This is equivalent to maximizing the ratio

$$\frac{\sum_{k=k_1}^{k_1+L-1} |a_k|^2}{\sqrt{L + 4L^{\frac{1}{2}} + 4}} \tag{84}$$

with respect to k_1 and L. Experimentally, it has been found that for most signals, the choice of L corresponds to the -3 dB bandwidth (-6 dB if there is a strong CW component at f_c), so a simple approximation for L is given by

$$L = \left\lfloor \frac{N\mathit{bw}}{f_s} \right\rfloor \tag{85}$$

where $\lfloor x \rfloor$ returns the nearest integer smaller than or equal to x, and *bw* represents the -3 dB bandwidth.

3.2 Polyphase Filter

One of the shortcomings of the FFT approach is that windowing reduces detection performance. However without windowing, the sidelobe performance of the FFT is quite poor (see Figure 6 or 7) so that detection of weaker hop signals in the presence of other stronger signals (hopping or conventional) can be problematic. Hence there is a trade-off between detection performance in the presence of noise, and detection performance in the presence of inband interference.

These limitations may be overcome by using FIR filters designed to produce a more ideal channel frequency response. The FIR filter equation for an $N\times P$-tap filter is given by

$$y(t) = \sum_{n=0}^{NP-1} x(t+n)h(n) \tag{86}$$

where $h(n)$ represents the filter coefficients. For each channel, a filter is desired which has the ideal response shown in Figure 9a and a normalized channel bandwidth of $1/N$. Using a separate filter for each frequency channel leads to a somewhat complicated arrangement. A simpler approach is to use a single low-pass filter and then frequency shift the data using a complex mixer before passing the data through the filter. The frequency shift is done so that each channel is shifted in turn to the low-pass filter band. Making these modifications to the filter equation, the search spectrum is given by

$$y_k(t) = \sum_{n=0}^{NP-1} x(t+n)e^{-j2\pi kn/N}h(n) \tag{87}$$

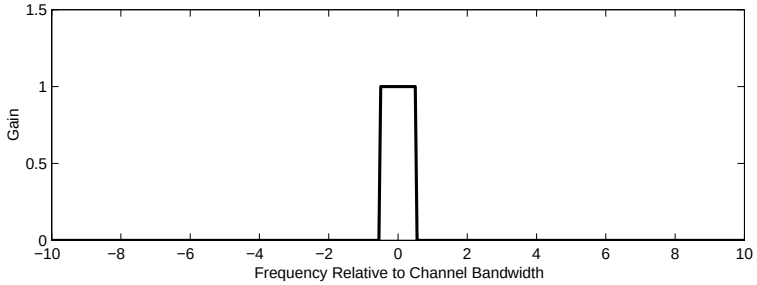

(a)

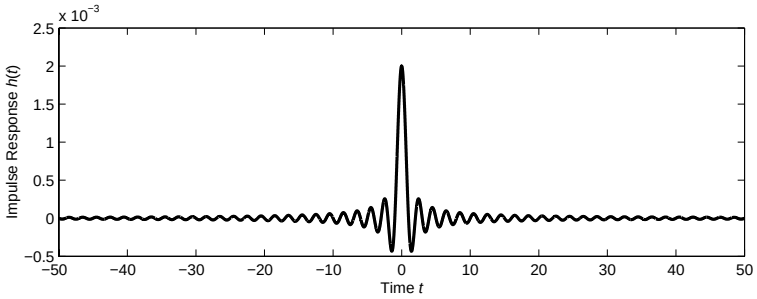

(b)

Figure 9: *Ideal channel filter response showing the (a) gain spectrum, and (b) the impulse response.*

Although there are many ways to compute the filter coefficients, one simple method follows from approximating the ideal channel filter response. The ideal impulse response of this filter is given by taking the inverse Fourier transform to get

$$\begin{aligned} h(t) &= \int_{-1/2N}^{1/2N} e^{j2\pi fn} df \\ &= \frac{1}{N}\text{sinc}(\frac{t}{N}) \end{aligned} \tag{88}$$

where $-\infty < t < \infty$. The impulse response is shown in Figure 9b for $-50 < t < 50$. Obviously, since this filter has an infinitely long impulse response, it is not useful for practical applications. For a finite data block of NP discretely sampled values, the ideal filter response can be approximated by quantizing and truncating the impulse response. Hence, centering the truncation around $t = 0$ for the best result, and assuming for simplicity that NP is even-valued, then for the discrete approximation the time index is restricted to

$$t = -NP/2 + 0.5,\ -NP/2 + 1.5, ..., -0.5, 0.5, ..., NP/2 - 1.5,\ NP/2 - 0.5 \tag{89}$$

This yields the discrete impulse response approximation given by

$$h(n) = \frac{1}{N} \text{ sinc} \left(\frac{1}{N}(n - \frac{NP}{2} + \frac{1}{2}) \right) \tag{90}$$

where $n = 0, ..., NP - 1$. The filter response can be further modified to reduce sidelobe and ringing effects by the application of a window function giving

$$h(n) = \frac{w(n)}{N} \text{ sinc}(\frac{1}{N}(n - NP/2 + 0.5)) \tag{91}$$

Two examples of the filter response for a polyphase filter are shown in Figure 10 where the filter coefficients were generated using (90), and (91) with a Blackman-Harris window. The polyphase filter response for either choice of coefficients is considerably superior to the FFT response shown in Figure 6.

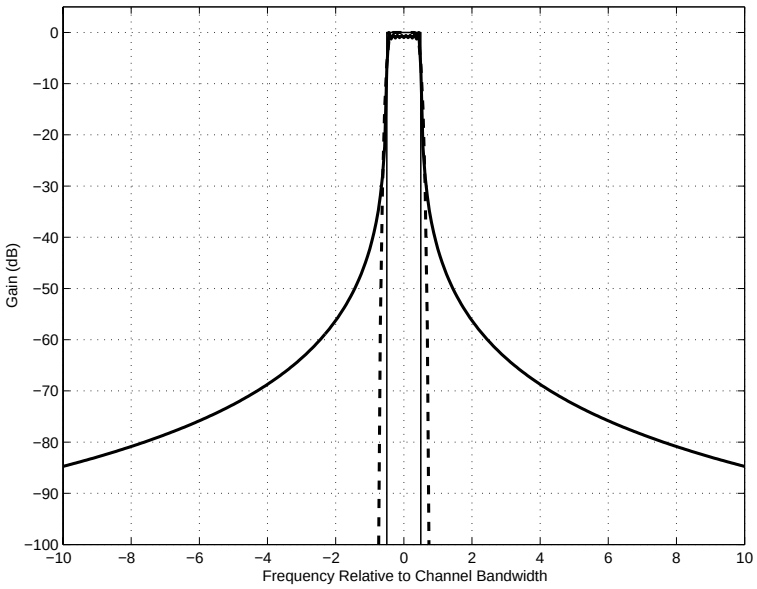

Figure 10: *Frequency response of the polyphase filter for the desired channel plus the ten adjacent channels on either side. The results were computed for* $(N, P) = (1024, 16)$*. The thick solid line shows the results when the filter coefficients were generated using no window, the dashed line shows the results when the Blackman-Harris window was used, and the thin solid line shows the ideal channel response.*

A useful feature of the polyphase filter approach is that if the filter equation is written out in the following manner

$$\begin{array}{ccccccc} & h(0)x(t) & + & ... & + & h(N-1)x(t+N-1)e^{-j2\pi k(N-1)/N} \\ + & h(N)x(t+N) & + & ... & + & h(2N-1)x(t+2N-1)e^{-j2\pi k(N-1)/N} \\ & \vdots & & & & \vdots \\ + & h(NP-N)x(t+NP-N) & + & ... & + & h(NP-1)x(t+NP-1)e^{-j2\pi k(N-1)/N} \end{array} \tag{92}$$

then it is evident that each row has the form of a Fourier transform. Hence, a more efficient way to compute the channel values $y_k(t)$ is to premultiply the data by the filter coefficients and then arrange the data in the same manner as above except *without* summing the data. The FFT is performed on each row in succession and the results from like FFT frequency bins are then summed together to give the N channel values $y_0(t), ..., y_{N-1}(t)$. Taking advantage of the FFT yields a large computational savings (assuming N is appropriately chosen), and is one of the main attractions of the polyphase filter approach.

For the purposes of detection, the polyphase approach has several advantages when compared to the FFT approach described in Section 3.1. In particular, losses due to windowing the data or mismatches of the hop signal frequency with respect to the center of the frequency channel, are considerably reduced. Windowing losses are compensated for by the larger amount of data used, while the improved channel passband response reduces the losses resulting from frequency mismatches or signal modulation. Additionally, the longer filter length (NP versus N for the FFT) allows for a much higher rejection of inband interference.

Noting the similarity between the expression for the channel outputs for the FFT, (28), and the corresponding expression for the polyphase filter, (87), the development of the expressions for the search spectrum, probabilities of false alarm and detection, and processing gain follow exactly the same approach. For the single channel processing approach, this leads to

$$S_{POLY_1}(f) = \sum_{n=0}^{NP-1} x(n)e^{-j2\pi fn}h(n) \tag{93}$$

$$PF_{POLY_1} = e^{-\tau^2} \tag{94}$$

$$PD_{POLY_1} = \frac{1}{2}\left(1 - \text{erf}(\alpha)\right) + \frac{1}{4\sqrt{\pi\beta snr}}e^{-\alpha^2}\left(1 - \frac{\alpha}{4\sqrt{\beta snr}} + \frac{1+2\alpha^2}{16\beta snr} - ...\right) \tag{95}$$

$$\tag{96}$$

and

$$\textit{Processing Gain} = 10\log\beta \text{ dB} \tag{97}$$

where $f = k/N$ for $k = 0, ..., N-1$, and

$$\alpha = \tau - \sqrt{\beta snr} \tag{98}$$

Additionally, the correlation time constant β is redefined for the polyphase case as

$$\beta = \frac{\beta_1^2}{\beta_2^2} \tag{99}$$

where

$$\beta_1 = \sum_{n=0}^{NP-1} h(n) \tag{100}$$

$$\beta_2 = \sqrt{\sum_{n=0}^{NP-1} h(n)^2} \tag{101}$$

An example of the value of β as a function of P is shown in Figure 11, which illustrates that $\beta \rightarrow N$ for increasing P. Interestingly, β exceeds N for all values of $P > 1$ so that the processing gain will also be greater than $10 \log N$; better detection performance than would be expected. However, this results from the channel bandwidth ($1/beta$) being smaller than $1/N$ (the desired bandwidth) for $P > 1$ so that less noise enters each channel. The negative consequence is that signals near the channel edges will be more heavily attenuated than desired, leading to poorer detection performance for these signals. The channel bandwidth problem can be corrected by modifying the filter coefficient equation (91) according to

$$h(n) = \frac{w(n)}{N'} \text{ sinc}(\frac{1}{N'}(n - NP/2 + 0.5)) \tag{102}$$

and then adjusting $N' > N$ until the channel bandwidth equals the desired bandwidth, or $\beta = N$.

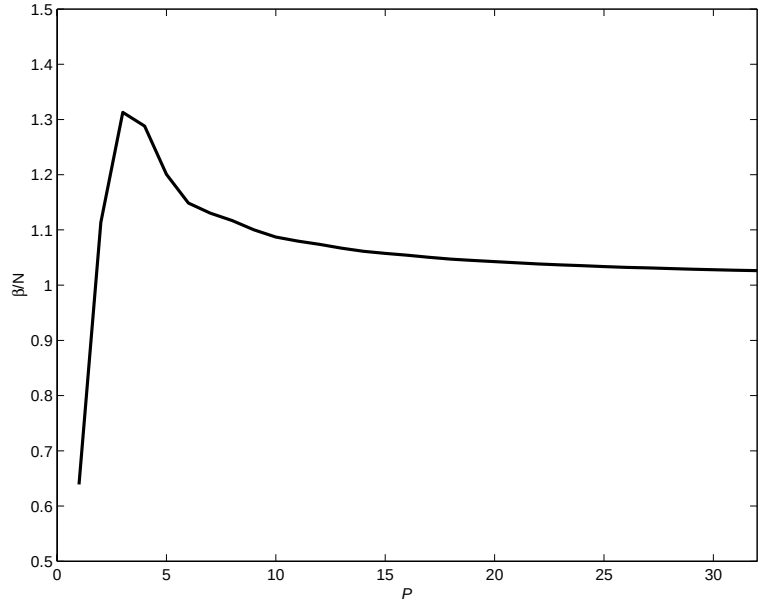

Figure 11: *Example of the change in the normalized value β/N as P increases. For this example, $N = 2048$ and a Hanning window was used.*

When frequency channel smoothing is used, the corresponding expressions are given by

$$S_{POLY_L}(f) = \sum_{n=k}^{k+L-1} \left| \sum_{n=0}^{NP-1} h(n)x(n)e^{-j2\pi kn/N} \right|^2 \quad (103)$$

$$PF_{POLY_L} = e^{-\tau^2 L} \sum_{k=0}^{L-1} \frac{\tau^{2k} L^k}{k!} \quad (104)$$

$$PD_{POLY_L} = \frac{1}{2} + \frac{1}{2}\text{erf}\left(\frac{\beta snr + L(1-\tau^2)}{\sqrt{2L + 4\beta snr}} \right) \quad (105)$$

and

$$\textit{Processing Gain} = 10\log\beta - 5\log L \ \text{ dB} \quad (106)$$

The same comments about adjusting the filter coefficients until $\beta = N$ also apply in the frequency smoothed case. The smoothing window size L can be determined either by maximizing (84), or calculating directly using (85).

4. Alternate Approaches

The previous section discussed detection methods which use sample sizes typically much shorter than a signal hop. Since it was shown in Section 2 that a maximum processing gain of $10\log(M)$ is possible, where M is the length of the hop, the use of small sample sizes leads to less than optimum performance. In this section, techniques to extend these small sample detection methods to much larger sample sizes are discussed, along with the ensuing performance benefits.

4.1 Periodogram

The periodogram uses the single channel FFT detection approach to sample multiple blocks of data as was illustrated in Figure 5. The spectrum for each of the individual blocks of data are then defined according to

$$S_{FFT_1}(t,f) = \sum_{n=0}^{N-1} w(n)x(n+t)e^{-j2\pi fn} \tag{107}$$

which is a modification of (35) explicitly showing the start time t of the current block being processed. The frequency is determined in the same way as before, namely, $f = k/N$ for $k = 0, 1, ..., N-1$.

Normally the values of t are chosen according to $t = 0, N_b, 2N_b, ...$, since it isn't usually necessary to compute the detection spectrum for every value of t. From the detection standpoint, the best choice of N_b is the minimum value for which the spectra generated from successive blocks are uncorrelated. Hence

$$N_b \;=\; \lfloor \beta \rfloor \;=\; \left\lfloor \frac{(\sum_{n=0}^{N-1} w(n))^2}{\sum_{n=0}^{N-1} w(n)^2} \right\rfloor \tag{108}$$

where β is the window correlation time constant discussed in Section 3.1.1 and previously defined in (44).

The periodogram spectrum is computed by combining the power spectrum from each block according to

$$S_{PER}(t,f) = \sum_{m=0}^{L-1} |S_{FFT_1}(f, t+mN_b)|^2 \tag{109}$$

where L is defined here as the number of blocks to be combined. To maximize detection performance, the number of blocks L is chosen so that $(L-1)N_b + N \approx M$. Assuming N_b is chosen according to (108), then the optimum number of blocks will be

$$L \;=\; \left\lceil \frac{M-N}{\beta} \right\rceil + 1 \tag{110}$$

where $\lceil x \rceil$ returns the nearest integer larger than or equal to x.

By inspection, it is apparent that the periodogram approach is conceptually similar to the frequency smoothing FFT approach, except the smoothing is done in time instead. Statistically, the analysis is the same except for the following modifications to (74) and (75)

$$E\{w\} = L\sigma^2\beta_2^2 + \beta_1^2 L\hat{a}^2 \tag{111}$$

and

$$VAR\{w\} = L\sigma^4\beta_2^4 + 2\sigma^2\beta_1^2\beta_2^2 L\hat{a}^2 \tag{112}$$

where $L\hat{a}^2$ replaces

$$\sum_{n=k}^{k+L-1} |b_n|^2 \tag{113}$$

The smoothing, in this case, is being done for one channel over time where the channel contains full signal power, rather than over L channels, where each channel contains only a portion of the signal power. Generally, $\hat{a} \leq a$, depending on frequency mismatch and modulation effects as discussed previously for the single channel FFT approach. Making these changes (or equivalently changing *snr* to *Lsnr* in the frequency smoothing expressions), the results are

$$PF_{PER} = e^{-\tau^2 L} \sum_{k=0}^{L-1} \frac{(\tau^2 L)^k}{k!} \tag{114}$$

$$PD_{PER} = \frac{1}{2} + \frac{1}{2}\text{erf}\left(\frac{\sqrt{L}(\beta snr + 1 - \tau^2)}{\sqrt{2 + 4\beta snr}}\right) \tag{115}$$

and

$$\textit{Processing Gain} = 10\log\beta + 10\log L - 5\log(L + 4L^{\frac{1}{2}} + 4) + 5\log 9 \text{ dB} \tag{116}$$

The extra $10\log L$ term is the additional processing gain that results from combining L spectra.

Note that the polyphase filter can also be adapted to the periodogram approach to take advantage of the superior channel filter response (e.g. lower sidelobes, faster roll-off in the transition from passband to stopband, and flatter passband response than compared to the FFT). The spectrum $S_{FFT_1}(t, f)$ is replaced by

$$S_{POLY_1}(t, f) = \sum_{n=0}^{NP-1} h(n)x(n + t)e^{-j2\pi fn} \tag{117}$$

but there are no other changes in (108)-(116).

4.2 Matched Frequency Smoothed FFT

The frequency smoothed FFT approach described in Section 3.1.2 can be matched to the hop signal by setting the block size equal to the hop duration and not using any windowing function. The actual choice of N may also depend on the FFT, but for simplicity, it is assumed that $N \approx M$. No windowing function is used since sidelobes have a faster decay rate relative to the signal bandwidth when the blocksize is increased, so for large enough blocksizes, windowing is unnecessary.

Making the appropriate changes to the expressions developed in Section 3.1.2, the time-frequency spectrum is computed using

$$S_{FFT_M}(t,f) = \sum_{m=k}^{k+L-1} \left| \sum_{n=0}^{M-1} w(n)x(n+t)e^{-j2\pi fn} \right|^2 \tag{118}$$

where $f = k/M$ and $k = 0, ..., M-L$.

The probability of false alarm, probability of detection, and the processing gain become

$$PF_{FFT_M} = e^{-\tau^2 L} \sum_{k=0}^{L-1} \frac{(\tau^2 L)^k}{k!} \tag{119}$$

$$PD_{FFT_M} = \frac{1}{2} + \frac{1}{2}\text{erf}\left(\frac{Msnr + L(1-\tau^2)}{\sqrt{2L + 4Msnr}} \right) \tag{120}$$

and

$$\textit{Processing Gain} = 10\log M - 5\log(L + 4L^{\frac{1}{2}} + 4) + 5\log 9 \ \text{ dB} \tag{121}$$

If the frequency spectrum of the signal is known, the smoothing size L can be estimated by maximizing

$$\frac{\sum_{k=k_1}^{k_1+L-1} |a_k|^2}{\sqrt{L + 4L^{\frac{1}{2}} + 4}} \tag{122}$$

with respect to k_1 and L. If only the 3 dB bandwidth of the signal is known, then

$$L = \left\lfloor \frac{Mbw}{f_s} \right\rfloor \tag{123}$$

In practical applications, the time index t will be chosen according to $t = 0, N_b, 2N_b, ...$ since $S_{FFT_M}(t,f)$ and $S_{FFT_M}(f, t+k)$ are correlated for $k < M$. Ideally, choosing $N_b = M$ would significantly reduce the number of computations required, but also increase the possibility that only 50% of a hop signal will be contained in any processed block of N data points, which would lead to a corresponding decrease in the processing gain. Extending this to any choice of N_b, the maximum drop in the processing gain will be given by

$$10\log(M - N_b)/M \quad \text{dB} \tag{124}$$

By setting a limit on this drop, then the value of N_b may be determined according to

$$N_b = \lfloor M(1 - 10^{\rho/10}) \rfloor \tag{125}$$

where $\rho < 0$ is the maximum degradation that can be tolerated in dB.

An example of the effective filter shape produced using a smoothing size $L = 33$ for a sample size of $M = 2^{15}$ is shown in Figure 12. The filter shape was produced by summing the power spectra response of the L individual channels. For comparison purposes, the response of a polyphase filter using a Blackman-Harris window and $(N, P) = (1024, 32)$, which gives $N \times P = 2^{15}$, has also been included. Additionally, to make comparisons easier, the channel bandwidth shown in the figure is the channel bandwidth of the polyphase filter, but L times the channel bandwidth of the frequency smoothed FFT approach (hence the term "synthetic channel").

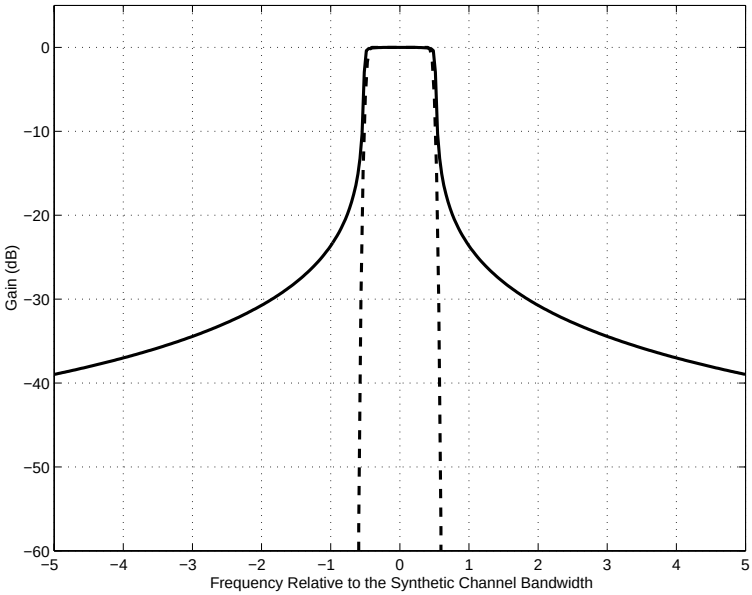

Figure 12: *Effective frequency response of the match frequency smoothed FFT filter (solid line) for $L = 33$ and $M = 2^{15}$ showing the desired synthetic channel (plus the ten adjacent synthetic channels on either side. The response for a polyphase filter (dashed line) using a Blackman-Harris window and $(N, P) = (1024, 32)$ is also shown for comparison purposes.*

Comparing the two filter responses, the frequency smoother FFT approach has a better passband response, but a poorer suppression of sidelobes in the stopband (note that for clarity, the variations in the stopband due to the sidelobes were smoothed out in the figure). The stopband performance is still considerably better than for the single channel FFT without windows (see Figure 6), and could be further improved by using a window (for the example shown in the figure, using a Blackman-Harris window leads to a response nearly identical to the polyphase filter response), but as discussed previously in Section 3.1.1, this degrades detection performance.

5. Comparative Results

5.1 Comparisons using a Simulated Signal

Although there has been discussion about the relative advantages of the various detection approaches throughout this report, it is useful to provide some comparative results which highlight comments made earlier. To do this, a simulated hop signal with additive white Gaussian noise was generated and the various detection methods were then tested using different levels of SNR and hop duration. The hop signal parameters are listed in Table 1, and the frequency spectrum is shown in Figure 13. The bandwidth listed Table 1 is the 3 dB bandwidth when the peaks at ± 5 kHz in the spectrum are ignored.

Table 1: *Hop signal parameters.*

Center Frequency	0 Hz (center of receiver band)
Modulation	FSK
Bandwidth	20 kHz
Bit rate	20 kb/s
Mark/Space Frequencies	± 5 kHz

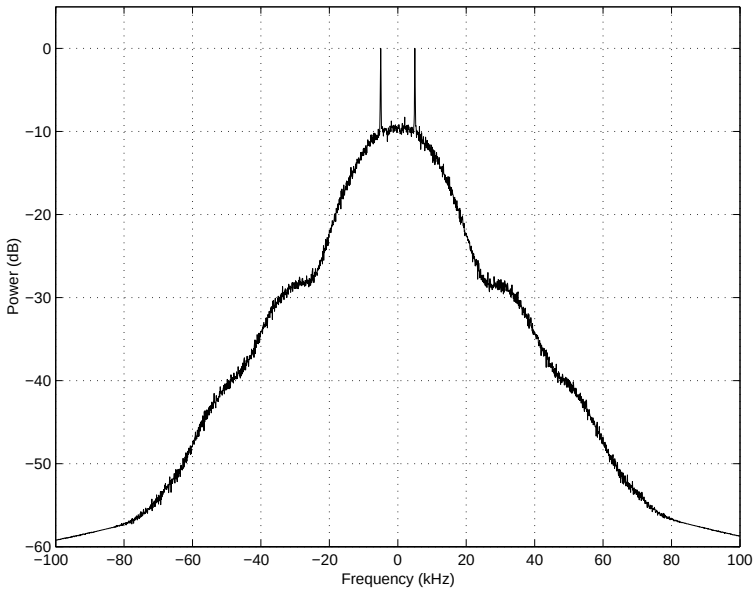

Figure 13: *Frequency spectrum of the FSK modulated hop signal used for testing.*

In addition to the signal parameters already listed, the hop duration was varied by doubling the sample size from $M = 2^{13}$ to $M = 2^{18}$, which, given a sampling rate of $f_s = 2.56$ MHz, corresponds to hop durations from 3.2 ms to 102.4 ms.

The various detection approaches that were used to process the data, and their associated parameters, are shown in Table 2. In the “Channels” column of the table, choosing 128 channels yields a channel bandwidth of 20 kHz which matches the signal

bandwidth. Choosing 1024 channels yields a smaller channel bandwidth requiring some frequency smoothing to be carried out. Finally, choosing M channels leads to the maximum amount of frequency smoothing. In the "L" column of Table 2, the smoothing parameter size was chosen according to (85) for frequency smoothing approaches (d), (f), (h), and (k), and according to (110) for periodogram approaches (i) and (j). In the "N_b" column, the block shift parameter for the periodogram approaches was chosen according to (108), and in the "P" column the choices of $P = 4$ and $P = 16$ for the polyphase approaches were made to show the effect of increasing P. Although not shown in the table, the detection threshold levels for each approach were set to give an expected probability of false alarm of 0.0001.

Table 2: *Detection approaches and their associated parameters.*

Detection Approach		Channels	Window Function	β	L	N_b	P
a	*ML*	M	–	–	–	–	–
b	*FFT*$_1$	128	none	128	–	–	–
c	*FFT*$_1$	128	Blackman-Harris	63.36	–	–	–
d	*FFT*$_L$	1024	none	1024	8	–	–
e	*Poly*$_1$	128	Blackman-Harris	161.99	–	–	4
f	*Poly*$_L$	1024	Blackman-Harris	1296.28	8	–	4
g	*Poly*$_1$	128	Blackman-Harris	138.58	–	–	16
h	*Poly*$_L$	1024	Blackman-Harris	1108.61	8	–	16
i	*Periodogram*	128	none	128	$M/128$	128	–
j	*Periodogram*	128	Blackman-Harris	63.36	$\lceil (M-128)/63.36 \rceil + 1$	63	–
k	*FFT*$_M$	M	none	M	$M/128$	–	–

For the simulations, the wideband data was created by generating a sample of the signal of length M and then adding a given level of white Gaussian noise. The approaches listed in Table 2 were then used to process that data. This was done 1000 times using new signal and noise samples each time after which the number of successful signal detections (out of 1000) for each approach was recorded. The noise level was incremented by 0.1 dB and the process repeated until the level had been determined at which a 0.9 probability of success occurred for each approach. This whole procedure was repeated for each value of M.

The results of the simulations for all approaches are shown in Table 3, for the case when $M = 2^{15}$. The results for the maximum likelihood, periodogram, and matched frequency smoothed FFT approaches are also shown plotted in Figure 14 as a function of M. The results for the periodogram approach with and without using the Blackman-Harris window were the same. The results for the other approaches are not shown in the figure since they did not vary as a function of M (which is expected since these approaches work on a fixed sample size regardless of the amount of data actually available).

The values of the detection SNR may also be calculated using the appropriate gain equations and the detection SNR for $M = 1$. The processing gain equations for the

Table 3: *SNR Results for a 12.8 ms hop with a probability of detection of 0.9.*

	Detection Approach	Detection SNR (dB)		Difference (dB)
		Simulated	Theoretical	
a	*ML*	-33.3	-33.4	0.1
b	FFT_1	-7.1	-9.3	2.2
c	FFT_1 (Blackman-Harris)	-6.3	-6.3	0.0
d	FFT_L	-15.9	-16.3	0.4
e	$Poly_1$ ($P = 4$)	-9.3	-10.3	1.0
f	$Poly_L$ ($P = 4$)	-16.2	-17.3	0.9
g	$Poly_1$ ($P = 16$)	-9.7	-9.7	0.0
h	$Poly_L$ ($P = 16$)	-15.1	-16.6	1.5
i	*Periodogram*	-23.8	-25.6	1.8
j	*Periodogram* (Blackman-Harris)	-23.7	-24.2	0.5
k	FFT_M	-24.6	-25.6	1.0

various approaches are summarized in Table 4. Using the target values of 0.0001 and 0.9 for the probabilities of false alarm and detection, respectively, the threshold value τ can be computed for the maximum likelihood approach using (15) and then *snr* can be solved numerically using (24) and (25) for $M = 1$. The result is *snr* $= 11.75$ dB. The predicted detection SNR for each approach is this value of *snr* (in dB) plus the processing gain calculated using the appropriate expression from Table 4. The predicted SNR values for the case when $M = 2^{15}$ are shown in the third column of Table 3.

Table 4: *Summary of processing gain equations.*

Detection Approach	Processing Gain Equation
ML	$10 \log M$
FFT_1	$10 \log \beta$
FFT_L	$10 \log \beta - 5 \log(L + 4L^{\frac{1}{2}} + 4) + 5 \log 9$
$POLY_1$	$10 \log \beta$
$POLY_L$	$10 \log \beta - 5 \log L$
Periodogram	$10 \log \beta + 10 \log L - 5 \log(L + 4L^{\frac{1}{2}} + 4) + 5 \log 9$
FFT_M	$10 \log M - 5 \log(L + 4L^{\frac{1}{2}} + 4) + 5 \log 9$

Looking at the differences between the predicted and simulated detection SNR levels (column four of Table 3, it can be seen that the theoretical levels were lower in most cases. This is because the processing gain equations were developed under the assumption that the signal was completely contained within a specific bandwidth. Inspecting Figure 13 this is clearly not the case, with 20% of the signal power outside the 20 kHz bandwidth. This corresponds to a decrease of 1 dB in the SNR of the signal when measured in the 20 kHz. The result is a similar increase in the detection SNR, although the actual change will depend on the filter characteristics of the given detection approach. For example, the single channel FFT approach using the Blackman-Harris window has an actual channel bandwidth of 40.4 kHz (instead of the desired 20 kHz) which means that a larger portion of the signal was available for

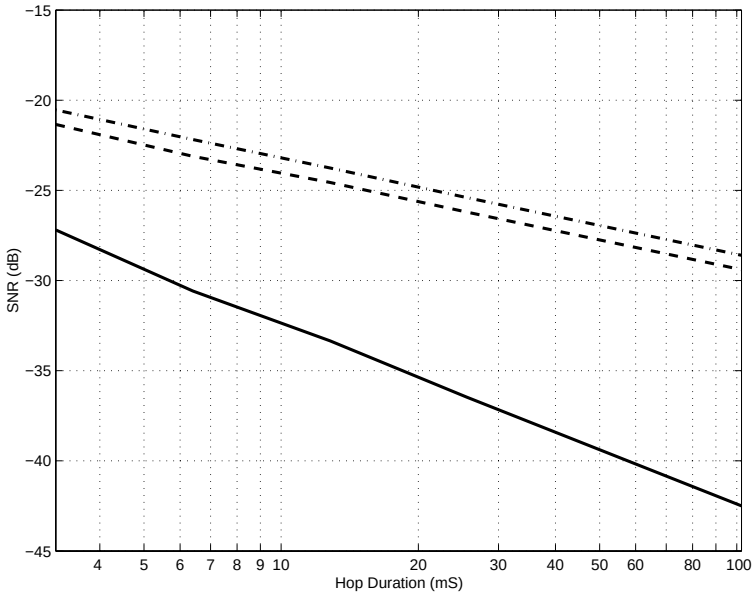

Figure 14: *Detection performance of the maximum likelihood (solid line), matched frequency smoothed FFT (dashed line), and the periodogram (dash-dot line), as a function of hop duration. The results are based on a probability of false alarm of 0.0001 and a probability of detection of 0.9.*

detection. As a result, the difference between the simulated and theoretical performance was smaller than 1 dB.

5.2 Number of Computations

The total number of computations required to process data using any of the approaches discussed in this report will depend on the actual implementation. Since it was not the intention of this investigation to determine the most computationally efficient implementations of these approaches, the assessment here is limited to the more obvious implementation schemes.

To make the comparisons useful, the input data is assumed to consist of T samples, where the duration of the target hop is much shorter than the duration of the sampled data ($M \ll T$), and the optimum number of channels for methods which do not use frequency smoothing is given by

$$N = \frac{f_s}{bw} \tag{126}$$

The number of computations required to generate the detection spectrum $|S(t,f)|$ for values of $t = 0, N_b, 2N_b, ..., \lfloor T/N_b \rfloor N_b - 1$ and $f = 0, 1/K, 2/K, ..., (K-1)/K$ where K is the number of channels . The squared detection spectrum $|S(t,f)|^2$ is substituted where it is computationally more efficient to do so (the corresponding detection threshold levels are also squared). The process to detect hops in the detection

spectrum $|S(t,f)|$ or $|S(t,f)|^2$ is excluded, since this process is presumed to be the same regardless of the detection approach. It is also assumed that various parameters chosen to implement each approach take full advantage of the FFT operation, which requires $K \log_2 K$ complex multiply-and-add operations to carry out.

Using these assumptions and guidelines, the number of computations for the single channel FFT approach for $t = 0$, can be represented by

$$xN + (x+y)N \log_2 N + xN \tag{127}$$

where "x" is used to denote complex multiply and "y" is used to denote complex add. The first term represents the application of windowing and disappears if windowing is not used. The second term is due to the FFT operation, and the third term is due the magnitude squaring operation to get $|S(t,f)|^2$. Repeating this operation for all T/N_b values of t, the total number of computations is

$$\textit{FFT}_1: \quad x\frac{2TN}{N_b}x + (x+y)\frac{TN}{N_b}\log_2 N \tag{128}$$

The optimal choice for the block shift parameter N_b is given by (108).

Performing a similar analysis on the single channel polyphase approach, the number of computations for $t = 0$ is represented by

$$xNP + (x+y)NP \log_2 N + yN(P-1) + xN \tag{129}$$

The first term represents the application of the filter coefficients, the second term represents the application of P FFT operations on data blocks of size N, the third term represents the addition of the results from the P FFT operations, and the fourth term represents the magnitude squaring operation to get $|S(t,f)|^2$. For all T/N values of t (where $N_b = N$), then the total number of computations is

$$xT(P+1) + yT(P-1) + (x+y)TP \log_2 N \tag{130}$$

which can be rewritten as

$$\textit{Poly}_1: \quad xT - yT + (x+y)TP \log_2 2N \tag{131}$$

The smoothing approaches require additional computations to calculate the smoothed spectral values. The smoothing operation can be represented by

$$S_k = s_k + s_{k+1} + ... + s_{k+L-1} \tag{132}$$

where S_k represents the smoothed spectral values for $k = 0, ..., N - L$ and s_k represents the unsmoothed spectral values. The first smoothed spectral value (computed for $f = 0$ for the frequency smoothed approaches and $t = 0$ for the periodogram

approach) requires $L-1$ complex adds. Subsequent smoothed values, however, may be computed by taking advantage of the relationship

$$\begin{aligned} S_k &= s_k + s_{k+1} + ... + s_{k+L-1} \quad (133) \\ &= S_{k-1} - s_{k-1} + s_{k+L-1} \quad (134) \end{aligned}$$

which demonstrates that only two complex adds are required for each new value of S_k when $k > 0$. Also noting that the frequency smoothing approaches use a greater number of channels ($K = N \times L$), the number of computations for the remaining approaches is given by

$$\textit{FFT}_L: \quad y\frac{-T(L+1)}{N_b'} \; + \; (x+y)\frac{TNL}{N_b'}\log_2 4NL \quad (135)$$

$$\textit{FFT}_M: \quad y\frac{-T(M+Nb)}{NN_b'} \; + \; (x+y)\frac{TM}{N_b'}\log_2 4M \quad (136)$$

$$\textit{Poly}_L: \quad y\frac{-T(L+1)}{N_b'} \; + \; (x+y)\frac{TNL}{N_b'}(1+P\log_2 2NL) \quad (137)$$

$$\textit{PER}: \quad yN(\frac{M}{N_b}-2) \; + \; (x+y)\frac{TN}{N_b} \; \log_2 4N \quad (138)$$

where $L = Mbw/f_s = M/N$ for the matched frequency smoothed FFT approach and $L = M/N_b$ for the periodogram was used. The choice of $N_b' \geq N$ for (135), (136), and (137) is determined using (125), and $N_b \leq N$ for (138) is determined using (108). The designation N_b' for the blockshift parameter differentiates it from the blockshift value N_b used for the single channel FFT or peridogram approaches, which is calculated differently.

Finally, the maximum likelihood approach can be implemented to take advantage of the FFT operation. Noting that for a fixed value of t, (3) has same form as the spectrum for the single channel approach given in (35), where the "window function" for the maximum likelihood approach is represented by $s^*(n-t)$. Hence the expression for the number of computations will be the same except that the number of channels is M (since $s(n)$ has M non-zero elements) instead of N. This yields

$$\textit{ML}: \quad x\frac{2TM}{N_b'} + (x+y)\frac{TM}{N_b'}\log_2 M \quad (139)$$

where N_b' is determined from (125).

In practical applications where a continuous stream of wideband data is being processed, $T \gg M \gg N_b \gg 1$, and the preceding expressions for the number of computations can be approximated by simpler expressions. Defining a computation as including a single complex multiply plus a single complex add, and normalizing by T (to make comparisons easier), the resultant expressions are shown in Table 5. Note that the results for the maximum likelihood and the windowed single channel FFT

approaches are based on the assumption that a single complex multiply counts as one half a computation (generally a multiply will count for more than this, but the results are machine dependent).

Table 5: *Number of computations for of various detection approaches.*

Detection Approach	$\frac{1}{T}\times$ (Number of Computations)
ML	$\frac{M}{N_b'}\log_2 2M$
FFT_1	$\frac{N}{N_b}\log_2 2N$
FFT_L	$\frac{NL}{N_b'}\log_2 4NL$
$POLY_1$	$1+P\log_2 2N$
$POLY_L$	$\frac{NL}{N_b'}(1+P\log_2 2NL)$
Periodogram	$\frac{N}{N_b}\log_2 4N$
FFT_M	$\frac{M}{N_b'}\log_2 4M$

Inspection of the expressions in Table 5 shows that the FFT operation (which gives rise to the $K\log_2 K$ term, where K is the number of channels) has a dominant effect on the processing time. Hence, approaches requiring a greater number of channels (i.e. the frequency smoothed approaches) are significantly slower.

For the polyphase approaches, the number of computations is directly proportional to P. For all the other approaches, the number of computations is inversely proportional to the blockshift parameter N_b.

The expressions shown in Table 5 for the single channel FFT approach, the frequency smoothed FFT approach, and the periodogram, all assume a window is being used. The main effect of windows is on the choice of N_b. The additional computations incurred by multiplying the data by the window values are relatively minor.

6. Conclusions

In this report, a number of approaches that can be applied to the problem of detection of a frequency hopped signal in digital wideband data were investigated both theoretically and through computer simulation. These approaches are listed in the first column of Table 6.

Table 6: *Relative assessment of detection approaches*

Detection Approach	Detection Performance	Sidelobe Suppression	Processing Speed
Single channel FFT with windowing	1	2	5
Single channel FFT without windowing	2	1	5
Single channel Polyphase	2	4	4
Frequency smoothed FFT	3	2	4
Frequency smoothed Polyphase	3	5	3
Periodogram	4	1	5
Matched frequency smoothed FFT	4	3	1
Maximum Likelihood	5	1	1

The main purpose of the investigation was to determine the best approach for detecting a frequency hopped signal in wideband data in the presence of noise. Detection performance was assessed by determining the lowest signal-to-noise ratio (SNR) at which a frequency hopped signal could still be observed. The lower this detection SNR, the better the performance. The relative detection performance of the approaches investigated is listed in the second column of Table 6 in increasing order, where 1 represents the poorest ability and 5 represents the best ability.

Generally, detection performance is related to the size of the observation window, i.e. the number of input samples used to make the detection assessment for a given time instance. The best performance is achieved when the observation window matches the hop duration, such as was done for the periodogram, matched frequency smoothed FFT (MFS-FFT), and maximum likelihood approaches. Although the ultimate performance was achieved using the maximum likelihood approach, it is not practical for communications applications since it requires knowing the exact modulation envelope of the signal. It was included, however, because it provides a useful performance standard by which other approaches may be gauged.

The investigation also highlighted other issues which have important practical implications. The first is sidelobe suppression. Sidelobes give rise to measurable signal power at frequencies outside the expected range of the signal. This unwanted signal power can mask weaker signals, making them impossible to detect. The relative sidelobe performance of the various approaches is listed in the third column of Table 6 (where 1 is used for the poorest suppression and 5 is used for the highest suppression). There are three methods that can be used to suppress the sidelobes: increase the FFT size, use a windowing function, or go to a polyphase filter technique. Using a

polyphase filter yields the greatest benefit, while increasing the FFT size can also be moderately effective. The use of windowing functions, unfortunately, leads to poorer detection performance.

The second issue is processing time. Processing time tends to be a function of the number of frequency channels used; the greater the number of channels, the longer the processing time. The result is that approaches employing frequency smoothing are slow, with the MFS-FFT approach being the slowest, since it involves the calculation of the largest number of frequency channels. The shortest processing time is required by the single channel FFT approach, followed closely by the periodogram approach, both of which also used the fewest number of frequency channels. Windowing functions for these two approaches lead to slightly longer processing times.

Generally the selection of the best detection approach for a given application results in a trade-off between performance and processing speed. In terms of processing speed, the FFT single channel or periodogram approaches with or without windows are the clear winners. For state-of-the-art wideband receiving system and realtime processing requirements, they may, in fact, be the only choices.

If detection performance is a greater consideration (and ignoring the maximum likelihood approach), the MFS-FFT and periodogram are the top choices. These detect frequency hopped signals at far lower SNR than any of the other approaches. For example, in simulations using a hop duration of 10 ms and a sampling frequency of 2.56 MHz, the differences were approximately 10-20 dB. Between the two approaches, the periodogram approach has the same or slightly worse detection performance than the MFS-FFT. Poorer detection performance occurs when a signal straddles two frequency channels (FFT bins). It becomes harder to detect since the noise power is doubled if both channels are considered in the detection process, or signal power is lost if only one channel is considered. The result is a loss of up to approximately 3 dB in performance (this problem is also common to all the approaches which don’t use frequency smoothing).

In terms of sidelobe performance, the polyphase approaches were the best, due to the much larger blocks of data that are used relative to the number of frequency channels. The single channel FFT and periodogram approaches were the worst. The sidelobe performance of MFS-FFT approach can be improved to a level equivalent to the polyphase based approaches by using a windowing function, but at the expense of some loss in detection performance.

Another consideration that may affect the choice of approach is integration with other applications. For example, the single channel FFT and polyphase approaches are wideband frequency channelizers whose output are also suitable for applications such as signal demodulation or spectral monitoring. If better detection performance is desired, it is also relatively straightforward to piggyback the periodogram approach onto a channelizer.

Additionally, from the ESM perspective, detection of a hop signal is not usually sufficient information. Estimation of hop parameters such as the hop signal bandwidth, start time, duration, and bearing are also of interest, so that the signal can be tracked in frequency and time. For example, the MFS-FFT approach has very good frequency resolution and intermediate results (i.e. the FFT output before frequency smoothing) could be used for accurate bandwidth estimation and discrimination between two signals closely spaced in frequency. The single channel FFT approach has poor frequency resolution, but much superior time resolution. Hence, choosing the most appropriate detection approach is not necessarily a straightforward process.

Compared to the ultimate performance of the maximum likelihood approach, the MFS-FFT and periodogram approaches still fall well short. For the example discussed previously (hop duration of 10 ms and sampling frequency of 2.56 MHz), the maximum likelihood performance was better by over 10 dB. Reducing the difference between practical performance and ideal performance may be possible by incorporating more information into the detection process. The MFS-FFT and periodogram approaches both assume that the hop signal bandwidth and duration are known. However, if a few hops have already been captured, it may also be possible to estimate the hop amplitude profile and the frequency profile, and incorporate this information into the detection process to improve performance. Alternatively, higher order statistical methods might also be incorporated to take advantage of the higher order statistical properties of man-made signals. In any case, more research needs to be done in this area to investigate and/or develop approaches which can provide improved frequency hop detection performance for practical ESM applications.

References

1. Leon-Garcia, Alberto, (1989). *Probability and Random Processes for Electrical Engineering*. Addison-Wesley Publishing Company, Reading, Massachusettes.

2. Rice, S.O., (1945). Mathematical Analysis of Random Noise. *Bell System Technical Journal*, 23, 282-332.

3. Harris, F. J., “On the Use of Windows for Harmonic Analysis with the Discrete Fourier Transform”, Proceedings of the IEEE, Vol. 66, No. 1, January 1978, pp 51-83.

4. Stremler, Ferrel G., (1977). *Introduction to Communication Systems*. Addison-Wesley Publishing Company, Reading, Massachusettes.

DOCUMENT CONTROL DATA

(Security classification of title, body of abstract and indexing annotation must be entered when the overall document is classified)

1. ORIGINATOR (the name and address of the organization preparing the document. Organizations for whom the document was prepared, e.g. Establishment sponsoring a contractor's report, or tasking agency, are entered in section 8.)

DEFENCE R&D CANADA -- OTTAWA
DEPARTMENT OF NATIONAL DEFENCE
OTTAWA, ONTARIO, K1A 0Z4

2. SECURITY CLASSIFICATION (overall security classification of the document, including special warning terms if applicable)

UNCLASSIFIED

3. TITLE (the complete document title as indicated on the title page. Its classification should be indicated by the appropriate abbreviation (S,C or U) in parentheses after the title.)

DETECTION OF FREQUENCY HOPPING SIGNALS IN DIGITAL WIDEBAND DATA (U)

4. AUTHORS (Last name, first name, middle initial)

READ, WILLIAM, J.L.

5. DATE OF PUBLICATION (month and year of publication of document)	6a. NO. OF PAGES (total containing information. Include Annexes, Appendices, etc.)	6b. NO. OF REFS (total cited in document)
DECEMBER 2002	44	4

7. DESCRIPTIVE NOTES (the category of the document, e.g. technical report, technical note or memorandum. If appropriate, enter the type of report, e.g. interim, progress, summary, annual or final. Give the inclusive dates when a specific reporting period is covered.)

DRDC OTTAWA TECHNICAL REPORT

8. SPONSORING ACTIVITY (the name of the department project office or laboratory sponsoring the research and development. Include the address.)

DEFENCE R&D CANADA -- OTTAWA
DEPARTMENT OF NATIONAL DEFENCE
OTTAWA, ONTARIO, K1A 0Z4

9a. PROJECT OR GRANT NO. (if appropriate, the applicable research and development project or grant number under which the document was written. Please specify whether project or grant)	9b. CONTRACT NO. (if appropriate, the applicable number under which the document was written)
5BB30	

10a. ORIGINATOR'S DOCUMENT NUMBER (the official document number by which the document is identified by the originating activity. This number must be unique to this document.)	10b. OTHER DOCUMENT NOS. (Any other numbers which may be assigned this document either by the originator or by the sponsor)
DRDC Ottawa TR 2002-162	

11. DOCUMENT AVAILABILITY (any limitations on further dissemination of the document, other than those imposed by security classification)

(x) Unlimited distribution
( ) Distribution limited to defence departments and defence contractors; further distribution only as approved
( ) Distribution limited to defence departments and Canadian defence contractors; further distribution only as approved
( ) Distribution limited to government departments and agencies; further distribution only as approved
( ) Distribution limited to defence departments; further distribution only as approved
( ) Other (please specify):

12. DOCUMENT ANNOUNCEMENT (any limitation to the bibliographic announcement of this document. This will normally correspond to the Document Availability (11). However, where further distribution (beyond the audience specified in 11) is possible, a wider announcement audience may be selected.)

UNLIMITED

13. ABSTRACT (a brief and factual summary of the document. It may also appear elsewhere in the body of the document itself. It is highly desirable that the abstract of classified documents be unclassified. Each paragraph of the abstract shall begin with an indication of the security classification of the information in the paragraph (unless the document itself is unclassified) represented as (S), (C), or (U). It is not necessary to include here abstracts in both official languages unless the text is bilingual).

In this report, a number of approaches to detect a frequency hopped signal in digital wideband data were investigated, both theoretically and through computer simulations. These approaches included the FFT, the polyphase filter, and the periodogram, plus variants of the these approaches using windowing functions and frequency smoothing. Additionally, the maximum likelihood approach was included as a benchmark for detection performance. The main purpose of the investigation was to determine the best approach for detecting a frequency hopped signal in wideband data in the presence of noise. The effect of interference from other inband signals was considered, and an assessment of the number of computations required for each approach was also carried out.

14. KEYWORDS, DESCRIPTORS or IDENTIFIERS (technically meaningful terms or short phrases that characterize a document and could be helpful in cataloguing the document. They should be selected so that no security classification is required. Identifiers such as equipment model designation, trade name, military project code name, geographic location may also be included. If possible keywords should be selected from a published thesaurus. e.g. Thesaurus of Engineering and Scientific Terms (TEST) and that thesaurus-identified. If it is not possible to select indexing terms which are Unclassified, the classification of each should be indicated as with the title.)

FREQUENCY HOPPING
ELECTRONIC SUPPORT MEASURED
ESM
MAXIMUM LIKELIHOOD
PERIODOGRAM
FFT
CHANNELIZATION
DETECTION

Defence R&D Canada

Canada's leader in defence
and national security R&D

R & D pour la défense Canada

Chef de file au Canada en R & D
pour la défense et la sécurité nationale

www.drdc-rddc.gc.ca